

# Optimization of Manufacturing Production and Process

*YinQuan Yu*

## Abstract

This chapter mainly introduces production processing optimization, especially for machining processing optimization on CNC. The sensor collects the original vibration data in time domain and converts them to the main feature vector using signal processing technologies, such as fast Fourier transform (FFT), short-time Fourier transform (STFT), and wavelet packet in the 5G AI edge computing. Subsequently, the main feature will be sent for cloud computing using genetic programming, Space Vector Machine (SVM), etc. to obtain optimization results. The optimization parameters in this work include machining spindle rotation velocity, cutting speed, and cutting depth, while, the result is the optimized main spindle rotation speed range of CNC, which met machining roughness requirements. Finally, the relationship between vibration velocity and machining quality is further studied to optimize the three operational parameters.

**Keywords:** machining processing optimization, time domain, short time Fourier transform, wavelet packet, genetic programming, deep learning

## 1. Introduction

The International Federation of Information Processing (IFIP) defines a numerically controlled (also commonly called CNC) machine tool as a machine tool equipped with program control. The difference between CNC machine tools and ordinary machine tools lies in the working sequence of NC machine tools: according to the requirements of part processing, CNC language is used to write processing sequences and parameter programs. After the program is analyzed and processed by the CNC device, the execution instructions are sent to the servo system to actuate the motion of the machine tool [1]. Programming controlled movement of the main spindle and worktable completes the processing that does not exist in ordinary machine tools. As shown in **Figure 1**, the mechanical aspects of CNC machine tools mainly include three major parts: the main shaft component [2], followed by the support component, and the conveying mechanism [3]. The main shaft is partially driven by a high-precision stepper motor or servo motor instead of a conventional motor. The transmission part uses a ball lead screw with less resistance and greater rigidity without backlash instead of the traditional lead screw. The CNC system controls the movement of the mechanical structure of the CNC machine tool to complete the processing of parts. The main component is the MCU. The coordination between its functions is an important index for evaluating the CNC machine tool and the CNC system [4].

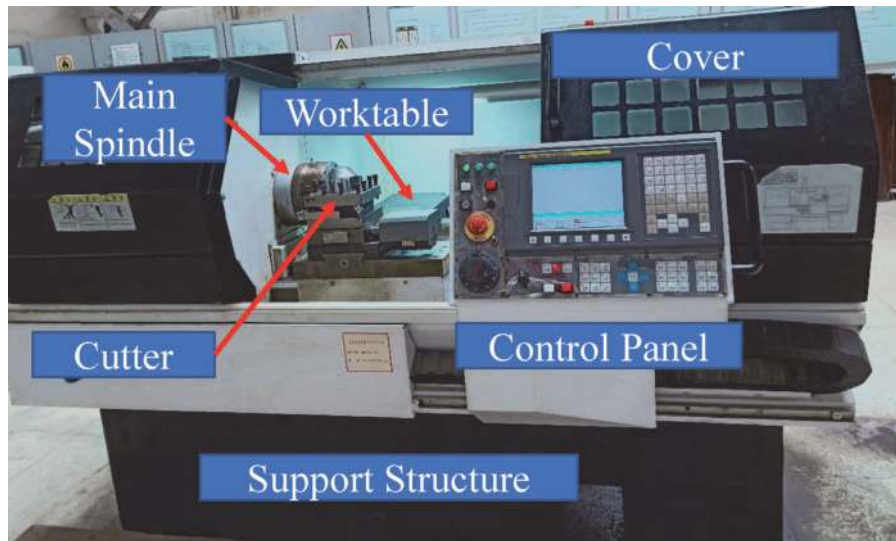


**Figure 1.**  
*Components of a CNC lathe.*

The optimization of CNC machine tools mainly includes the following three aspects:

### 1.1 Mechanism optimization

Improving machining accuracy of the machine tool must start from the design stage of the NC machine tool, adopt the drive device with outstanding dynamic performance, and use advanced control technology to improve anti-interference ability of the servo system [5–9]. Structural optimization design can calculate the durability and maintainability of NC machine tools, and design reliability by calculating the space error model of XYZ CNC machine tools by first-order and second-order matrices, Monte Carlo method, etc. [10]. By studying the kinematic configuration of CNC machine tools, it is found that it directly affects the nonlinear errors generated in the process of free-form surface machining [11], and has a direct impact on processing energy consumption and design of the supporting CNC system [12]. The moving parts of CNC machine tools and the mechanism of each feed axis also have a significant impact on the overall rigidity [13], positioning error [14], maintainability [15], and other indicators of CNC machine tools, which determine machining accuracy and work reliability [16]. The spindle of CNC machine tools can be analyzed and optimized by finite element analysis [17]. The finite element modeling can appropriately simplify some chamfers, small holes, etc. that do not affect mechanical properties [18]. The denser and more accurate the finite element (FEM) mesh division, the longer the optimization calculation time [19]. The method of selecting the appropriate unit division, which is not discussed here, can be found in ANSYS-related books. In addition to the influence of the spindle of the CNC machine tool, the deformation of the CNC machine tool due to insufficient static stiffness [20] causes deviations between the actual position and the ideal position of the tool and the workpiece, and seriously affects its machining accuracy. The guide rail has a decisive influence on the accuracy of the machine tool [21]. The optimized design of the guide rail of the machine tool can significantly improve the geometric accuracy of the bed rail, thereby significantly enhancing the

machining accuracy of the NC machine tool. Furthermore, selecting the right load rail by speed can optimize the machining quality. In terms of precision machining, a reasonable milling process should be selected according to different materials [22]. Choosing a suitable processing tool and enhancing the strength of the processing tool can avoid vibration caused by the high speed of the machine tool spindle during processing, which will affect processing accuracy [23]. For example, in the process of boring bar technology processing, strong heat treatment technology can be used to improve the rigidity and strength of its material. The error of the tool during manufacturing and machining wear [24] requires us to monitor it in real time to detect problems in time, check and integrate and summarize these problems, and then establish an error compensation model through the data system [25]. The influence of tools and bearings on the accuracy of machine tools is obvious [26]. The machining process should select the tool based on the cutting degree, depth, and accuracy of the parts [27], and the bearing selection should use bearings with relatively low friction resistance and high degree of smoothness and stability. During gear machining, the accuracy of the machine tool will affect transmission characteristics during gear machining [28–30]. The machining process can be regarded as the cutter wheel axis revolving around the center axis of the production wheel. Cogging is processed by 3–7 groups of tools. After each cogging is processed, the workpiece rotates and the next cogging is processed. Cutting tools installed on the tool turret includes outer blade, middle-outer blade, middle-inner blade and inner blade. There are three main methods to check the machining accuracy of CNC machine tools [31]: sample detection method, indirect detection method [32], and direct detection method.

## **1.2 Energy consumption optimization**

The energy-saving process optimization of CNC machine tools usually divides the machine tool's energy consumption into several parts [33]; the auxiliary system, the main drive system, the feed system, and the process of cutting and load. Gaussian process regression models are established according to these five parts, and the differential evolution algorithm is used to optimize the model. According to the processing requirements, a model of the energy consumption, cost, and time of the cutting process is established. The dynamic multi-swarm particle swarm optimization algorithm is used for calculation to obtain more diverse and convergent results [34]. The energy consumption of CNC milling machines can be divided into three parts, namely fixed energy consumption, no-load energy consumption, and milling energy consumption [35]. It can analyze the multi-source energy flow of the machine tool and the energy consumption of the machining process to establish the power of the machining stage equations and energy consumption estimation models. The calculation of energy consumption can be carried out from the amount of cutting, processed gears, cutting tools, cutting fluids of CNC machine tools, etc. to study carbon emissions [36]. The finished processing time is then established. The machining surface accuracy and other conditions are based on the reduction of carbon emissions from the spindle speed and feed rate during machining. A multi-objective optimization model for optimizing carbon emissions and processing costs can be established [37], which can be solved by genetic algorithms [38], and the feasibility of the optimization method of the model is verified by simulation calculation. On the digital intelligent machine tool, a system for detecting the energy consumption of the machining process of the CNC machine can be designed based on the upper computer information interaction unit and the lower computer information acquisition element.

### **1.3 Process optimization**

The process design optimization of CNC machine tools has a significant impact on their precision performance. The design of the machining process of the machine tool should determine the processing steps and clamping methods of the workpiece by analyzing the mechanical drawings of the parts; the geometric elements of the outline of the part, the accuracy requirements of the dimensional tolerances, the accuracy requirements of the shape and position tolerances, surface smoothness requirements, material quality requirements, and the number of processes mode [33]. The feed route, choice of cutting amount, and choice of tool can then be determined. In order to prevent the tool from colliding with the workpiece during the machining process, the optimization of the machining process must be carried out by interference avoidance research [39, 40]. Based on the algorithm of coordinate extremes, the complex surface should be simplified by taking an arc of the surface [41], and performing measurement on the bisector. The vibration of the machine tool gravely affects its machining accuracy [42]. The hardness and thickness of the workpiece during the machining process [43] and the force of the machine tool are taken into consideration [44]. For the movement path [45], the movement speed [46] is optimized to achieve the machine vibration damping control. Another vibration reduction method is passive vibration reduction, which using materials with strong vibration resistance strengthens the stability of CNC machine tools [47]. Another factor affecting the machining accuracy of CNC machine tools is thermal deformation. During the working process of the machine tool, the moving parts of the machine tool will be affected by thermal deformation, which will cause relative displacement between the tool and the workpiece [48]. The solution is to strengthen cooling and lubrication during the work process to reduce the displacement [49]. The thermal characteristics, machining environment, and specific cutting parameters of the machine tool determine the size of the thermal error by solving the function of the time-varying temperature field under given conditions [50]. The purpose of the auxiliary heat source is to balance the temperature field to reduce heat source interference. In short, the errors caused by structural deformation, vibration, and high temperature in CNC machine tools can be compensated with the following methods: single error synthesis compensation technology [51], geometric error direct compensation technology, geometric error synthesis compensation technology [14], single-term error synthesis compensation technology by studying the error produced by a certain CNC machine tool, and geometric error direct compensation technology by measuring the error data to directly error compensation on the CNC machine tools. Using geometry error synthesis compensation technology, the unidirectional error information is decomposed by obtaining the synthetic error value of the CNC machine tool. It is particularly important to emphasize the tremendous difficulty in accurately measuring the angular error of the spindle during the general process; however, it can now be solved by a matrix using a laser interferometer [52]. For complex curved surface processing, multi-step compensation must be adopted as follows: (1) pre-compensation; (2) error detection; and (3) reverse compensation. For the deformation of the tool during machining, mirror image anti-deformation compensation that mirrors the tool position point and the tool axis vector must be adopted [53].

To sum up, the reliability of CNC machine tools is guaranteed by the processing quality of each part of the CNC machine tools, and the quality of processed parts is controlled by the quality of the processing procedures. For the analysis of the machining process of the machine tool, it is necessary to analyze the machining process of a key part. The optimization parameters of CNC machine tool machining process are mainly energy consumption during machining, machining efficiency,

and machining accuracy. Due to the limited space, this chapter only discusses the influence of optimization parameters on machining accuracy.

## 2. CNC common processing optimization approach

The Computer Numerical Control (CNC) machine tools lie in the working principle of CNC machine tools: according to the requirements of part processing and using CNC language, the processing sequence is written into parameter programs, and the program is analyzed by Multipoint Control Unit (MCU). After processing, the execution instructions are sent to the Driving System of step motors or Servo motors and the machine tool will start machining the work piece. The position and velocity signals of the machine tool will then be sent back to the MCU. The schematic of CNC is shown in **Figure 2**.

From a mechanical point of view, CNC machine includes three main sub-systems: the main spindle sub-system, followed by the supporting sub-system and the conveying mechanism sub-system. From a control point of view, it mainly includes two sub-systems: Data Processing Unit and Control Loop Unit. The processing of parts action is completed through the numerical control system by controlling the mechanical structure of the CNC machine tool. The coordination between their functions is an important index for evaluating the machine tools under the CNC system. To fully utilize the merits of CNC for precision machining, a reasonable milling process should be selected according to different materials. Vibration caused by excessive rotation speed of the machine tool spindle will affect machining accuracy. The outer ring can be processed after specific processing. During the process of boring bar technology, thermal stiffness enhancement technology can be used to improve the rigidity and strength of the material.

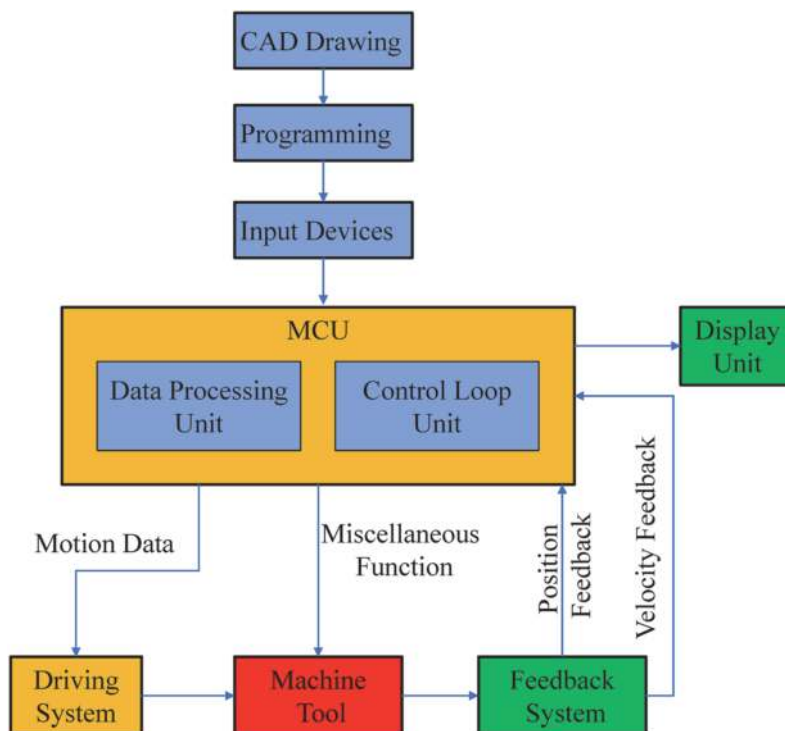


**Figure 2.**  
*Schematic diagram of CNC.*

## 2.1 Cutting force monitoring

To obtain the wear and tear errors in the manufacturing and processing of cutting tools, we need to monitor them in real time to detect problems in time, check, integrate, and summarize them, and then establish them through the data system error compensation model. The deformation of the machine tool due to insufficient static stiffness, which causes deviations between the actual position and the ideal position of the tool and the workpiece, seriously affects its machining accuracy. In Precision Machining process on CNC, the cutting force in tangential and radial directions needs to be predicted based on monitoring signals and machining process parameters such as cutting depth, cutting width, rotational speed of the main spindle, and feed speed of the cutting tool. The experimental data of the cutting forces are shown in **Figure 3**.

## 2.2 Processing path optimization

The kinematic configuration of CNC machine tools directly affects the nonlinear errors generated in the process of free-form surface machining, and has a direct impact on processing energy consumption and design of the supporting CNC system.

After determining the motion configuration of the CNC machine tool, the mechanism of each feed axis has a significant impact on the overall rigidity, positioning error, maintainability, and other indicators of the CNC machine tool, which determine its machining accuracy and work reliability. For instance, in order to machine complex surface S12, it needs to be decoupled into surface S1 and S2. According to the required feed motion of surface S1 and S2, we can get the feed motion of combined curved surface S12 as shown in **Figure 4**.

A heuristic algorithm (HA) is one that is designed to solve a problem in a faster and more efficient fashion than traditional methods at the expense of optimality, accuracy, precision, or completeness. Although it has the capability of convergence and obtaining the optimization result efficiently, it depends heavily on initial result and may only obtain local optimal solution of non-smooth curve functions. Moreover, it occupies a large amount of computing resources and has a poor real-time performance, which may be incompatible with Computer Aided Manufacturing (CAM) on CNC. In order to overcome this issue, a discrete tool planning is proposed as follows:

$$Path = \left\{ (A, C)_{path_1}^1, (A, C)_{path_2}^2, (A, C)_{path_3}^3, \dots, (A, C)_{path_m}^m \right\}. \quad (1)$$

where,  $(A, C)_{path_m}^m$  represents the positions of two rotary feed axes A and C when the cutting point is on m.

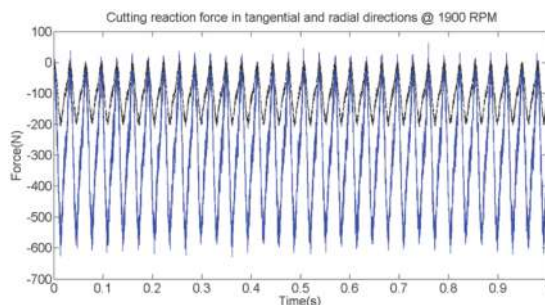


**Figure 3.**  
The experimental cutting forces in tangential and radial directions.

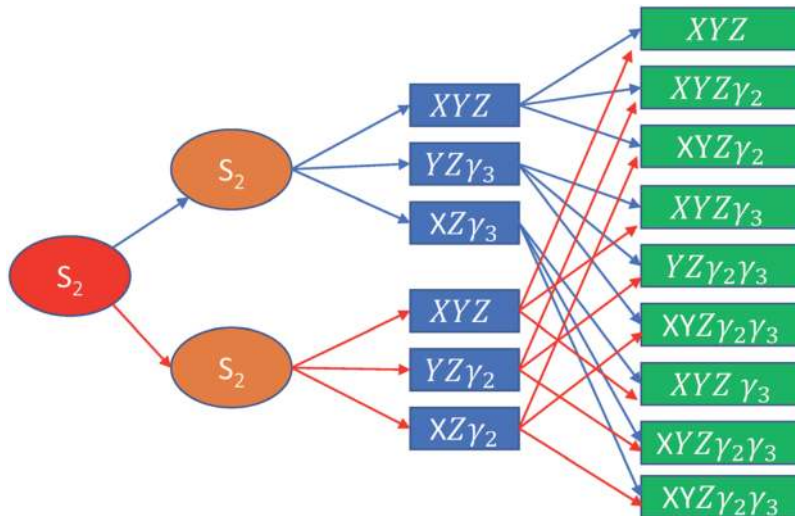


**Figure 4.**  
 The feed motion of  $S_{12}$  obtained from that of decoupled surface  $S_1$  and  $S_2$ .

One methodology for positioning error compensation of CNC machine tools is through interpolation. It produces third-order splines from the coordinates of discrete points measured by Laser Doppler velocimetry (LDV). Between  $[x_{i-1}, x_i]$ , the interpolation function of splines  $s(x)$  can be deduced as

$$s(x) = \frac{[(x_i - x)^3 * M_{i-1} + (x - x_{i-1})^3 * M_i]}{6h_i} + \left( y_{i-1} - \frac{h_i^2}{6} * M_{i-1} \right) \frac{x_i - x}{h_i} + \left( y_i - \frac{h_i^2}{6} * M_i \right) \frac{x - x_{i-1}}{h_i}, i= 1, 2, \dots n \quad (2)$$

In order to obtain  $M_{i-1}$ , let

$$\begin{cases} d_i = \frac{6}{h_i + h_{i+1}} \left( \frac{y_{i+1} + y_i}{h_{i+1}} - \frac{y_i + y_{i-1}}{h_i} \right) = 6f'(x_{i-1}, x_i, x_{i+1}) \\ u_i = \frac{h_i}{h_i + h_{i+1}}, \lambda_i = \frac{h_{i+1}}{h_i + h_{i+1}} = 1 - u_i \end{cases} \quad (3)$$

Since the binomial multi-order derivative is continuous,  $M_i$  satisfies  $N - 1$  equations,

$$u_i M_{i-1} + 2M_i + \lambda_i M_{i+1} = d_i \quad i = 1, 2, 3 \dots, n - 1 \quad (4)$$

The first type of boundary conditions is

$$S'(X_0) = f'_0 = m_0, S'(X_n) = f'_n = m_n \quad (5)$$

Then, Eq. (4) can be present as

$$\begin{bmatrix} 2 & \lambda_0 & & & \\ \mu_1 & 2 & \lambda_1 & & \\ & \dots & \dots & \dots & \\ & & \mu_{n-1} & 2 & \lambda_{n-1} \\ & & & \mu_n & 2 \end{bmatrix} \begin{bmatrix} M_0 \\ M_1 \\ \dots \\ M_{n-1} \\ M_n \end{bmatrix} = \begin{bmatrix} d_0 \\ d_1 \\ \dots \\ d_{n-1} \\ d_n \end{bmatrix} \quad (6)$$

### 2.3 Processing dynamic profile optimization

To prevent CNC machining in normal condition, the acceleration and velocity of the moving stages have to be monitored and should be less than the maximum design range of CNC machine.

With the known coordinates of two adjacent track points  $(x_{n+1}, z_{n+1}), (x_n, z_n)$  and the velocity of the main spindle, the acceleration and velocity of point n are approximately.

$$\Delta t = \frac{\Delta \theta}{\omega}, v_n = \begin{bmatrix} \frac{x_{n+1} - x_n}{\Delta t} \\ \frac{z_{n+1} - z_n}{\Delta t} \end{bmatrix}, a_n = \begin{bmatrix} \frac{\dot{x}_{n+1} - \dot{x}_n}{\Delta t} \\ \frac{\dot{z}_{n+1} - \dot{z}_n}{\Delta t} \end{bmatrix}. \quad (7)$$

Figure 5 shows the monitored acceleration in x and z directions respectively. Their values should be within CNC machine design range. NC machining process usually faces “over cutting” issue, which can be minimized through the commonly used method of rotating the tool angle as shown in Figure 6.

The extreme value  $S_t$  and root mean square value  $S_q$  of the machining surface shape are the two major indicators of the machining accuracy and are calculated by the following equations:

$$S_t = \max(e) - \min(e), S_q = \sqrt{\sum_{i=1}^n e_i^2/n}. \quad (8)$$

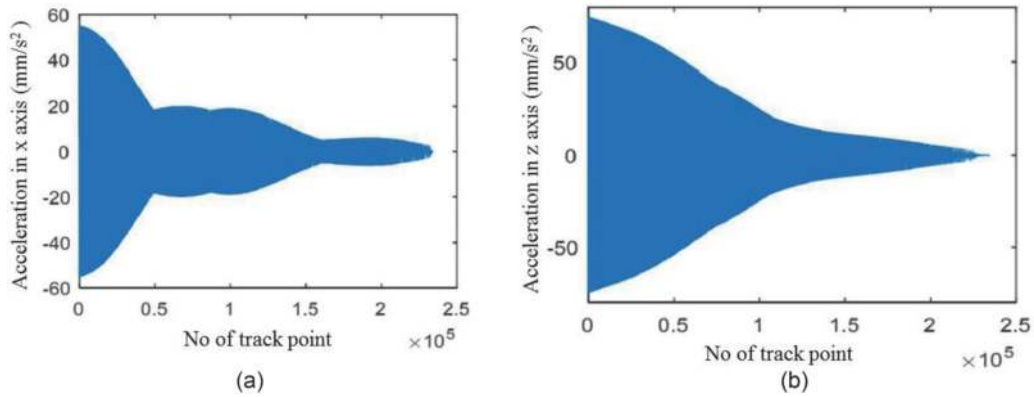


Figure 5. Discrete point acceleration of machining trajectory. (a) Acceleration of track pint in x axis and (b) acceleration of track pint in x axis.

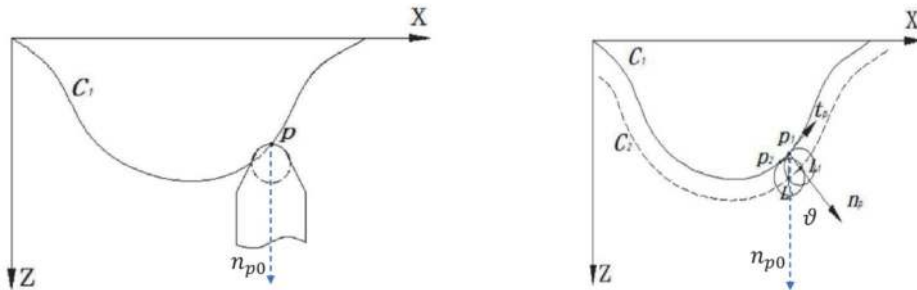


Figure 6. Machining tool overcutting compensation.



where  $e$  represents the shape tolerance of the machining surface,  $N$  represents the number of the measured point.

**Figure 7** shows the implementation of cutting tool compensation to reduce the machining error. It can be seen that tool compensation can effectively solve machining errors from 0.8 to 0.5  $\mu\text{m}$  due to overcutting of tools through rotating cutting tool angle  $\vartheta$ .

To minimize the value of  $S_{-}(t)$  and  $S_{-}(q)$ , the optimized machining profile should be conducted as shown in **Figure 8**. In order to make the movement of the machine tool smooth and the processing more stable, the concept of “jerk” is introduced and made as constant. Then, the profile of acceleration is trapezoid. It can be seen that the speed profile of trapezoid acceleration is smoother than that of constant acceleration. As we know that the reaction force of the worktable and feed screw becomes infinite if the acceleration is suddenly changed. As a result, it may damage some motion transmission parts of CNC, such as worktable, lead screw, or servo motor.

Usually, in order to obtain high quality of the machining parts and extend the working life of the CNC machining, the speed of CNC is kept as constant as possible besides start and end stage of the machining processing.

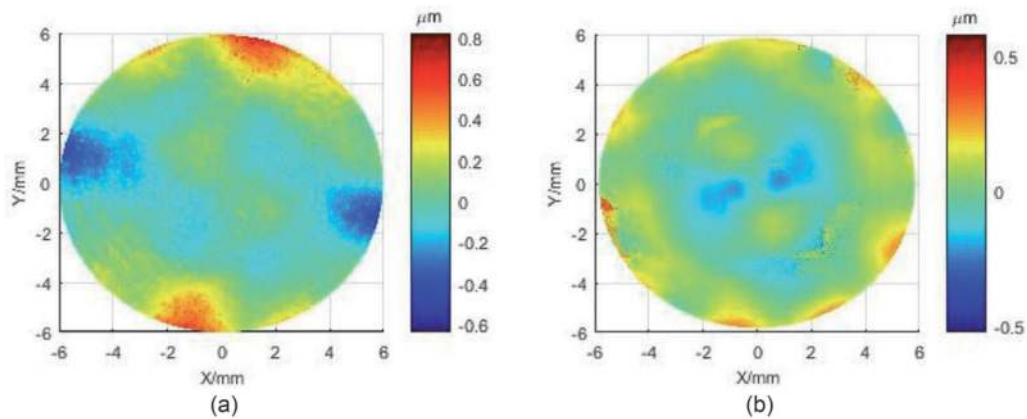


**Figure 7.** Cutting tool compensation to reduce machining error. (a) Machining error before tool compensation and (b) machining error after tool compensation.

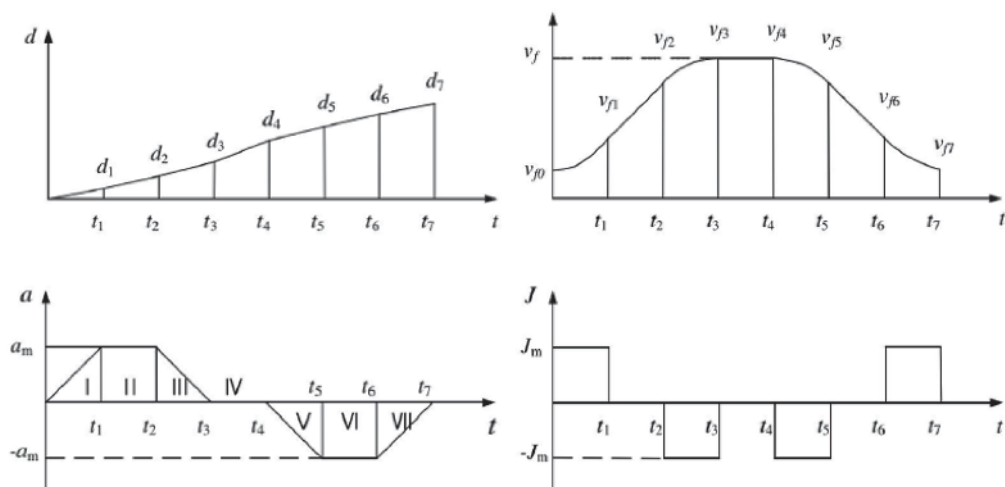


**Figure 8.** Distance, velocity, acceleration, jerk vs. time profile in acc/dec process of CNC machining.

### 3. Processing tools deflection compensation

Any machining process will induce dynamic reaction forces on the cutting tool. Cutting tool deflection due to improper clamping, tool wear, and error in machine accuracy may lead to error in the final product. Hence, the current trend in the industry is to detect such errors and compensate for them in machining to avoid scraping the material afterward. In this chapter, we attempt to detect the cutting tool deflection while machining the workpiece and hence predict error on the workpiece. To detect the deflection during machining, we use either a contact or a non-contact sensor. One of the major considerations in choosing the right sensor is cost and ability to measure the error under harsh environments. In this section, compared to capacitive probe, we finally decide to adopt eddy current gap sensors to detect deflection of the cutting tool during machining of a simple profile and predict error on the workpiece. The predicted error was then verified using Coordinate Measuring Machine.

#### 3.1 Displacement sensor for tool compensation

To compensate for the cutting tools or work piece deflection, there are two types of commonly used displacement sensors to monitor: (1) capacitance gap sensors and (2) Eddy current type gap sensors.

##### 3.1.1 Capacitance gap sensors

The capacitance of a parallel-plate capacitor is given by

$$C = \frac{\epsilon_r \epsilon_0 A}{d} \quad (9)$$

where,  $\epsilon_r$  represents electric constant of the insulating medium ( $\epsilon_r = 1$  for air);  $\epsilon_0$  represents permittivity of air or vacuum, which is  $8.85 \times 10^{-12}$  F/m; A represents overlapping area in plates; and d represents varying distance between the bottom surface of the electrode of capacitive probe and the surface of measured object (tool cutting tip).

The working schematic of the capacitive probe is shown in **Figure 9(a)**. It is evident that changes in the distance between the capacitive probe and the measured object (cutting tools) change the capacitance, which in turn changes the current flow in the sensing element. RF oscillator generates 500 kHz and 1 MHz high-frequency electric field to focus the sensing field on the cutting tool. **Figure 9(b)** shows the relationship between distance d and capacitance c. It shows d decreases as c increases. Based on this principle, the distance between plates can be determined by calculating the capacitance value.

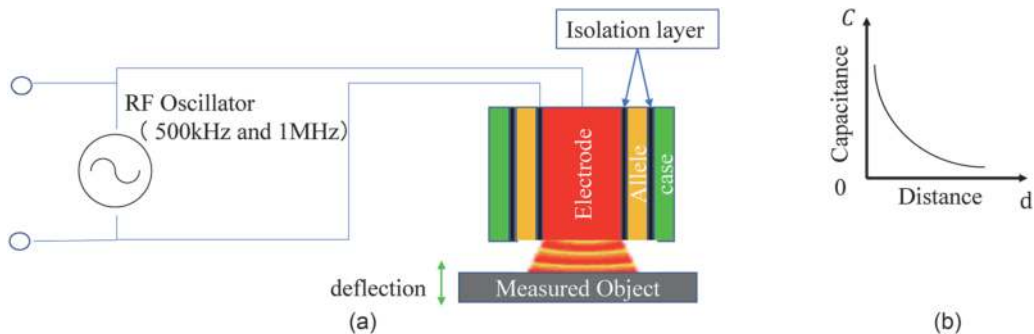


**Figure 9.** The working schematic and principles of capacitive probe. (a) Schematic of capacitive probe and (b) capacitance vs. distance.

### 3.1.2 Eddy current type gap sensors

The working schematic of eddy current gap sensor is shown in **Figure 10**. When a nonmagnetic conductive target material is introduced into the coil field, eddy currents are induced on the target's surface. These currents generate a secondary magnetic field, inducing a secondary voltage in the sensor coil. The result is a decrease in the coil's inductive reactance (the coil-target interaction is similar to the field interaction between the windings of a transformer). By calculating the "effective impedance" of the sensor coil, the distance to the target can be determined.

Nonmagnetic conductive target materials (e.g., aluminum, copper, brass, gold), with low resistivity and a magnetic permeability of 1, can provide output sensitivity in terms of impedance change per unit of target displacement.

The capacitive probe is suitable for measuring any metal surface. Its measuring accuracy can reach up to several nanometers. However, the dusty working environment is not suitable for applying capacitive probe to measure the target, as the gap between probe and the measured target is contaminated by dust, liquids such as coolant. As a result, the measuring accuracy of the capacitive probe is affected. On the other hand, the current gap sensor is suitable for measuring conductive material except steel. However, it cannot measure thin materials because of insufficient eddy current generated, thus affecting the measuring accuracy of the gap sensor.

### 3.2 Tool deflection compensation approach

**Figure 11** shows 5G AI Edge computing configuration for CNC cutting tool deflection compensation. The original signal is collected by sensor and sent to 5G AI computing for preprocessing such as noise reduction with low-pass filter, compressed data etc. The dimension-reduced data is sent for cloud computing through a 5G network router. The cloud computing device uses genetic programming (refer to **Figure 12**) to generate the cutting tool deflection compensation algorithm and sends it back to the 5G AI edge computing local network. 5G AI edge computing device then calculates the compensation value and sends it to MCU to compensate for the cutting tool deflection.

### 3.3 Algorithm adopted in tool deflection compensation

Genetic programming (GP) is adopted in this study to conduct tool deflection compensation. It evolves from computer programs that are traditionally represented in memory as tree structures. Trees can be easily evaluated in a recursive manner. Every tree node has an operator function and every terminal node has an operand, rendering mathematical expressions easy to evolve and evaluate. Thus, traditionally GP favors the use of programming languages that naturally embody tree structures.

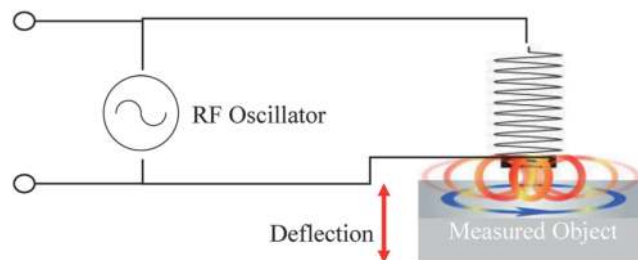


**Figure 10.**  
*The working schematic of eddy current gap sensor.*

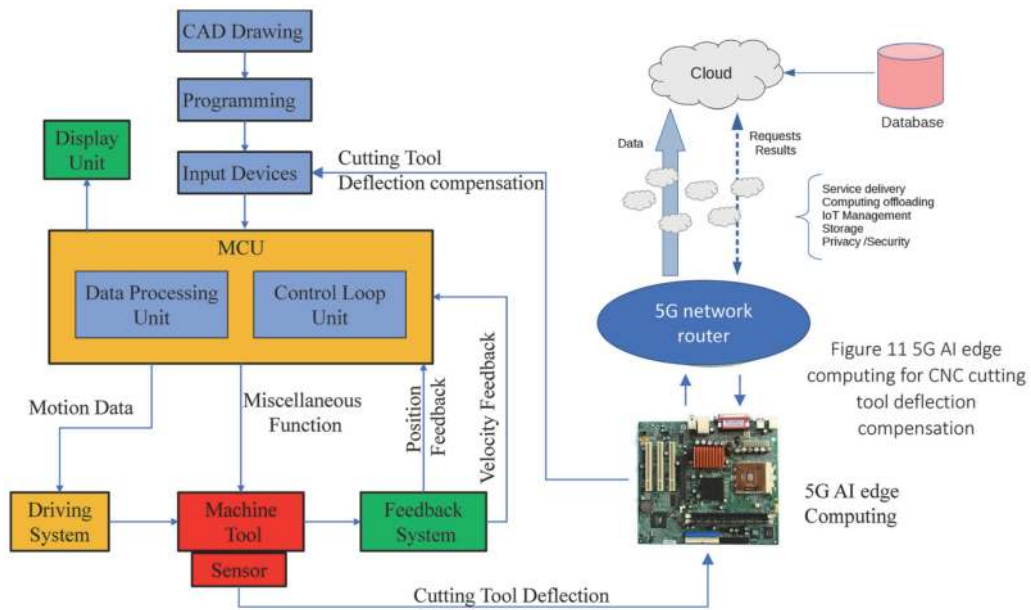


**Figure 11.**  
5G AI edge computing for CNC cutting tool deflection compensation.

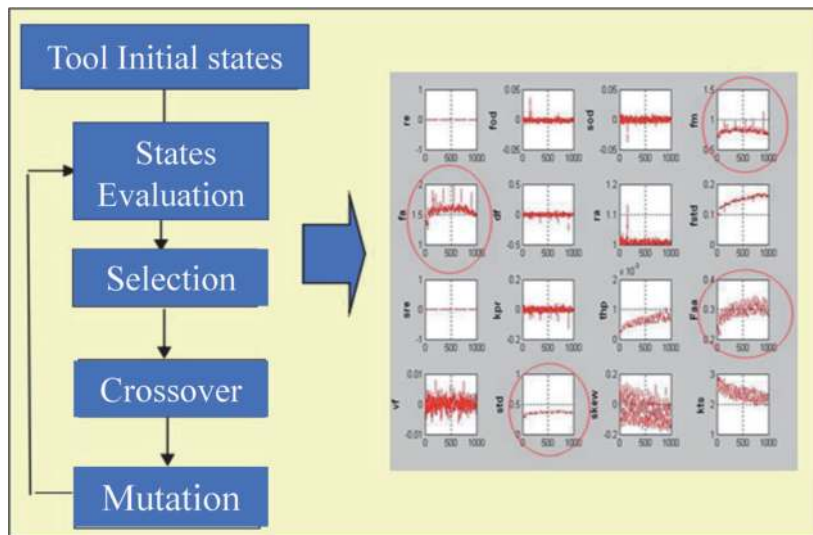


**Figure 12.**  
Schematic of genetic programming for tool deflection compensation.

GPLAB is a genetic programming toolbox for MATLAB® initially developed by Sara Silva. The main modules of GPLAB are GENPOP, GENERATION, and SETVARS. GENPOP module generates the initial population and calculates its fitness based on default or user defined fitness function. Terminal set:

**Terminal set:** “X1,” “rand,” and “100”.

**Terminal condition:** Maximum generation reached.

**Function set:** plus (+), minus (-), times (\*) and other protected function in.

**Fitness function:** Fitness function is defined as the minimum value between actual value and predicted value. During the programming calculation process, the new population should be superior to the previous population. In other words, the new fitness value will be lower than previous one.

$$\text{Fitness} = \min (\text{abs} (\text{predicted result} - \text{expected result})). \quad (10)$$

The schematic of genetic programming for tool deflection compensation is shown in **Figure 12**. The optimal tool deflection compensation algorithm is obtained through hundreds of generation selection, crossover, and mutation operation until set fitness function is reached.

### 3.4 Tool deflection compensation experiment

The material of cutting tools includes high-speed steel, ELMAX chromium-molybdenum-vanadium alloy steel, or nickel-chromium alloy steel. However, the cutting chip will reduce the capacitive probe measurement sensitivity and accuracy and damage the capacitive probe. Therefore, the eddy current gap sensor will be adopted in this working environment. The deflection signal is sent to 5G AI edge computing for signal pre-processing, before sending for computing through genetic programming. The computing results are sent back to MCU of the CNC to control the movement of the main spindle and the worktable.

The cutting surface error compensation with and without cutting tool deflection compensation are shown in **Figure 13**. It shows that the maximum machining error

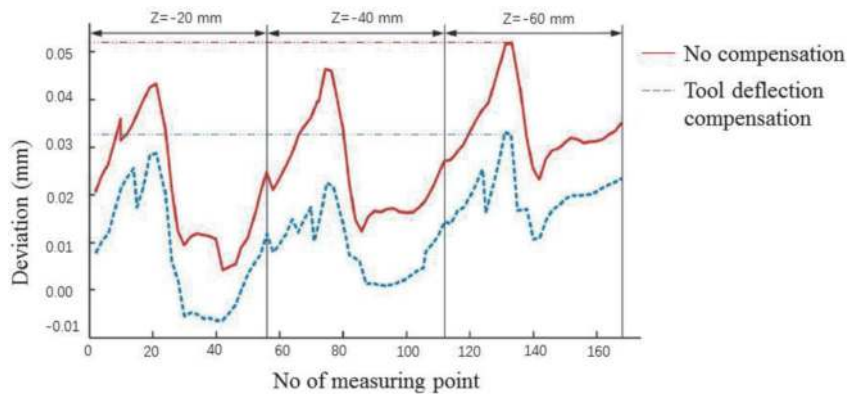


**Figure 13.**  
*Cutting surface error with/without tool deflection compensation.*

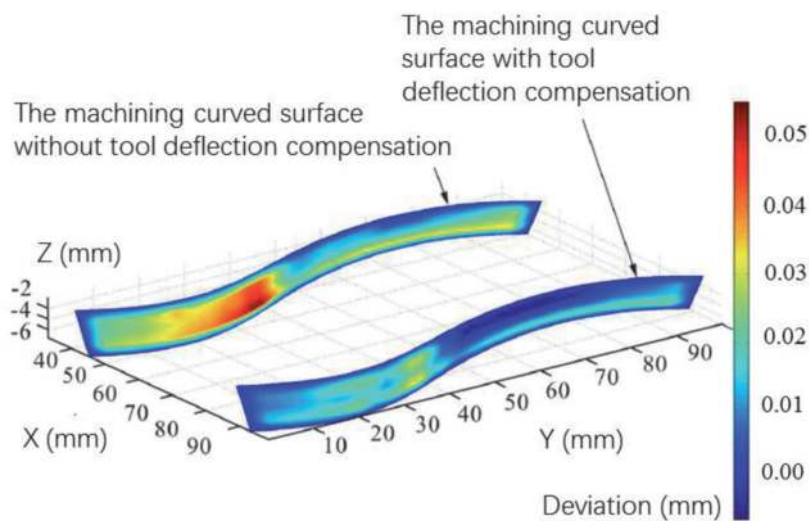


**Figure 14.**  
*The deviation distribution of the machining with/without tool deflection compensation.*

is reduced from 0.053 to 0.032 mm, which is 40%. The deviation distribution of machining with/without tool deflection compensation is shown in **Figure 14** in three dimensions. It can be seen that at almost all measured points, the machine error on a curved surface without tool deflection is larger than that on a machining curved surface with tool deflection compensation. Moreover, the error is largest at the bottom area of inflection of the curved surface, reaching 0.053 mm. This may be due to two reasons. First, the cutting tool suffered the largest reaction force and induced the largest deflection. Second, the stiffness of the machining tool is smallest at the tip.

## 4. Processing error feedback compensation

### 4.1 Experimental setup of error feedback compensation

In order to further reduce the machining error after cutting tool compensation, the error feedback compensation strategy is selected as shown in **Figure 15**. Two accelerometers are attached to the side of the stator of the main spindle and the side of the workpiece to measure their vibration signals respectively. The vibration of the accelerator attached to the main spindle in idle and working conditions is monitored and feedback to CNC, then, the CNC control the main spindle rotation speed to obtain minimum vibration signal. The vibration sensor attached to the workpiece monitored the dynamical performance of the workpiece and the signal is sent back to the control unit for processing. A servo actuator is attached to the bottom surface of the workpiece to compensate for the machining error, which is based on control signal received from control unit. An acoustic emission sensor is attached near the workpiece to monitor the acoustic noise and the fault processing condition. The original signal is sent to control main server for processing and pattern and status recognition. Lastly, the control command is sent from the main server to CNC machine to minimize the machine error.

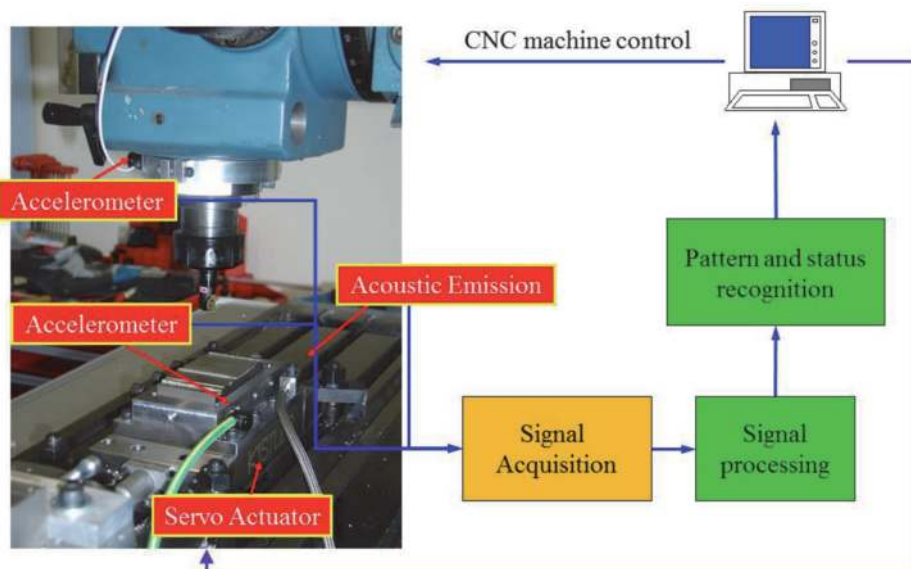


**Figure 15.**  
*Schematic of error feedback compensation.*

## 4.2 Signal processing in error feedback compensation

**Figure 16** shows error feedback compensation signal noise filter and reconstruction processing. The original time domain signal is obtained from the vibration sensor and converted into frequency domain through fast Fourier transform (FFT) algorithm. The bandpass filter is applied to filter out high frequencies and low-frequency and DC component. Interesting frequencies that include useful information are obtained after applying a signal technology to find peaks of the FFT in the range. The final step is to reconstruct the signal to control the actuator in order to compensate for machining error.

## 4.3 Experimental results of error feedback compensation

**Figure 17** shows the cutting surface error without tool deflection compensation, with tool deflection compensation, and with error feedback compensation. It can be seen that the maximum machining error is reduced by 35% from 0.032 to 0.021 mm when the error feedback compensation is applied. Therefore, the total machining error is reduced by 60% from 0.53 to 0.021 mm. However, the error feedback strategy does not work at measurement point 40. Moreover, in two ranges (point 20–28, point 45–55), machining error is larger than that with tool deflection compensation strategy only.

The deviation distribution of machining without compensation, with tool deflection compensation, with error feedback compensation is shown in **Figure 18**. It can be seen that the deviation distribution of the machine curved surface with feedback compensation is minimal. On the other hand, the deviation distribution of the machine curved surface without tool deflection and error feedback compensation is largest. In other words, in order to achieve good machining quality product, the tool deflection compensation and error feedback compensation strategy should be adopted.

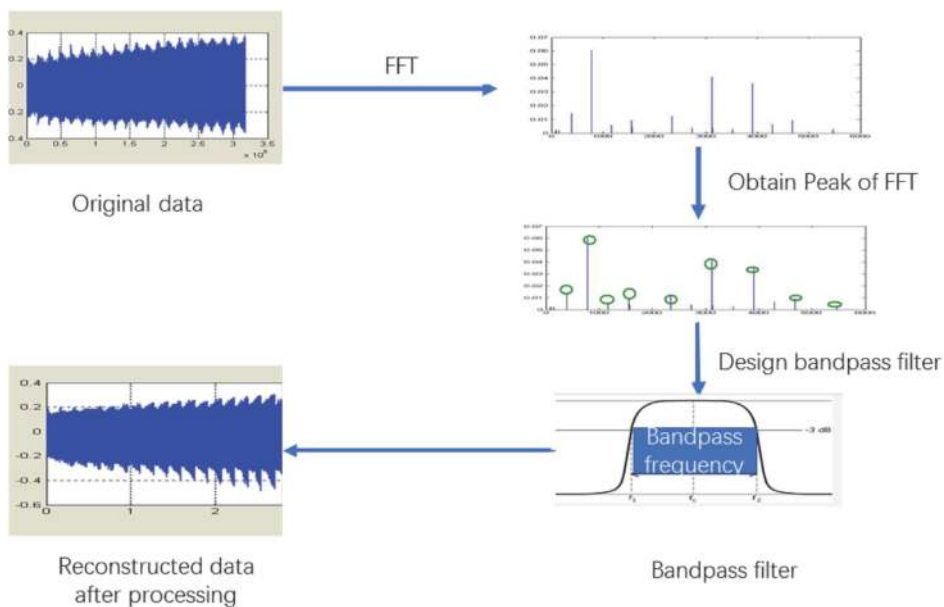


**Figure 16.**  
*Error feedback compensation signal noise filter and reconstruction processing.*

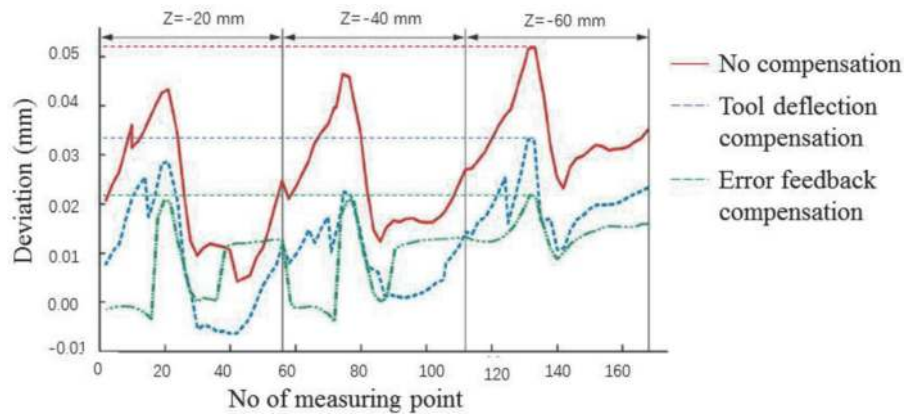


**Figure 17.** The machining surface error without tool deflection compensation, tool deflection compensation, error feedback compensation.

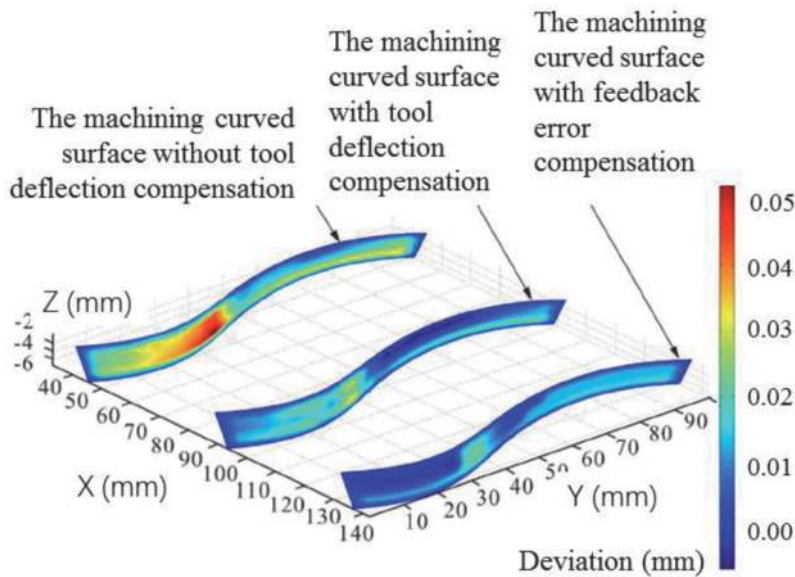


**Figure 18.** The deviation distribution of the machining without compensation, with tool deflection compensation, with feedback error compensation.

## 5. Processing parameter optimization compensation

An experienced operator can significantly reduce machining error by applying cutting tool deflection and error feedback compensation when the optimized operation parameter is known. However, the process obtaining optimized operation parameter by try and error is time-consuming for new operator. Therefore, this section will introduce the parameter base optimization operation strategy. 5G AI edge computing and cloud computing strategy will be applied to obtain optimized operation parameter automatically.

### 5.1 Network configuration for processing parameter optimization

**Figure 19** shows the cloud-based intelligent manufacturing configuration with 5G AI edge computing, which is also known as smart manufacturing configuration. The company data center managed by the IT department acts as a data transfer



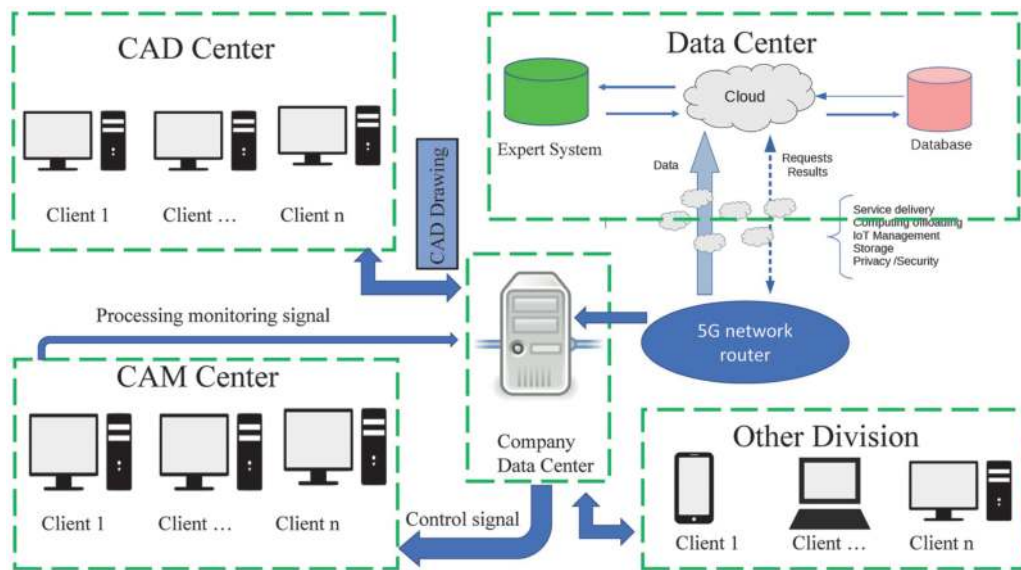


**Figure 19.**  
*The cloud-based intelligent manufacturing configuration.*

bridge connecting each department of the company such as CAD center, CAM center, sales department, supply department, warehouse, maintenance department etc. It also acts as a data communication buffer linked to cloud computing centering out of the company. The designer can access the local data center to download the CAD drawing in order to modify the existing drawing, save the new CAD drawing, or update drawing to local data center. In the CAM center, every client computer is connected to a CNC machine. The CNC machine processing monitoring signal and the corresponding machine number information are sent to the company data center and to the cloud computing data center if necessary. All information needed for CAM center to produce the machining parts is sent through company data center as well. For instance, the production manager can download the CAD drawing from company data center and convert it to CAM file format. The technical person from the company then sends a file with control command or a file with the new compensation algorithm trained by cloud computing to the client PC in the CAM center. Cloud computing center receives request and the training data set from the company and sends back the proposed processing optimized parameters or processing control algorithm. In the cloud data center, the data received from the company will be stored in a database. It utilizes GP, MNRR, or other deep learning algorithm to obtain the optimized parameters through the expert system.

**Figure 20** shows the cloud-based intelligent manufacturing configuration in the CAM center. The whole system configuration includes CNC real-time machining status monitoring, real-time environmental monitoring, CNC cutting tool deflection compensation, error feedback compensation as well as CNC machining operation process optimization through a combination of cloud computing and 5G AI edge computing. Unlike traditional standalone CNC machining, all CNC machines (refer to **Figure 21**) are connected through a local network client PC with cable or wireless in intelligent manufacturing environment. CAD drawing is sent to a local client instead of programming. The signals from sensors monitoring the CNC machining status are sent to 5G AI edge computing devices to pre-process. Processed data and corresponding machine no. are sent to the company data center through the client PC.

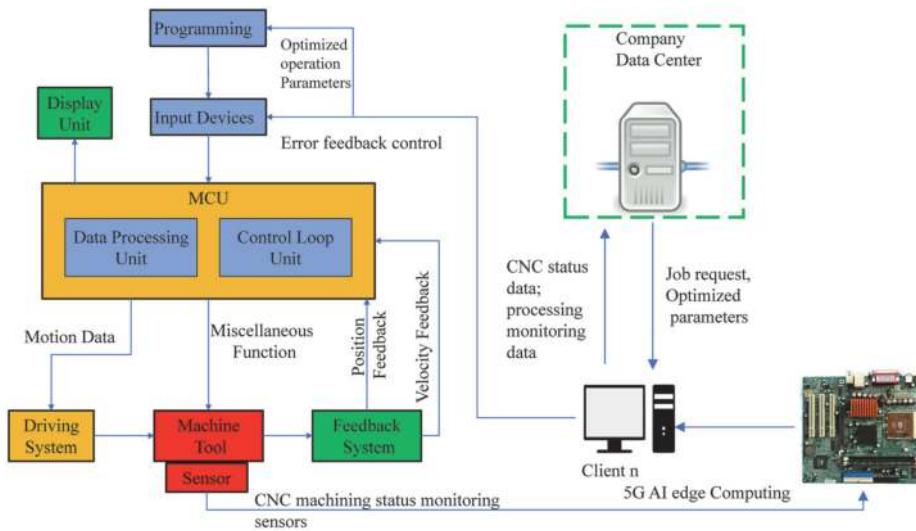


**Figure 20.**  
The cloud-based intelligent manufacturing configuration in CAM center.



**Figure 21.**  
A group of CNC machines connected through local networks.

## 5.2 Data collection for processing parameter optimization

**Figure 22** shows a CNC machine connected to the local network. In order to obtain vibration signal to train the GP, Neural Networks (NNR), and Support Vector Machine (SVM) algorithm, two wireless accelerometers, Sensor 1 and Sensor 2, are attached to the cutting tool. Their signals will be sent to the cloud for GP, NNR, and SVM base computing. Specimen (Nylon) is clamped into three-jaw chuck. Vibration signal is sent to cloud server through 5G AI Edge computing device and 5G router. In order to find optimized operational rotational speed of main spindle, three groups of specimens (30 pcs) are machined with varied rotational speed as shown in **Tables 1–3**.

In order to get reliable data, the three groups of specimens must have the same experimental condition; the diameter and length of all experimental specimens are 25 and 30 mm respectively.

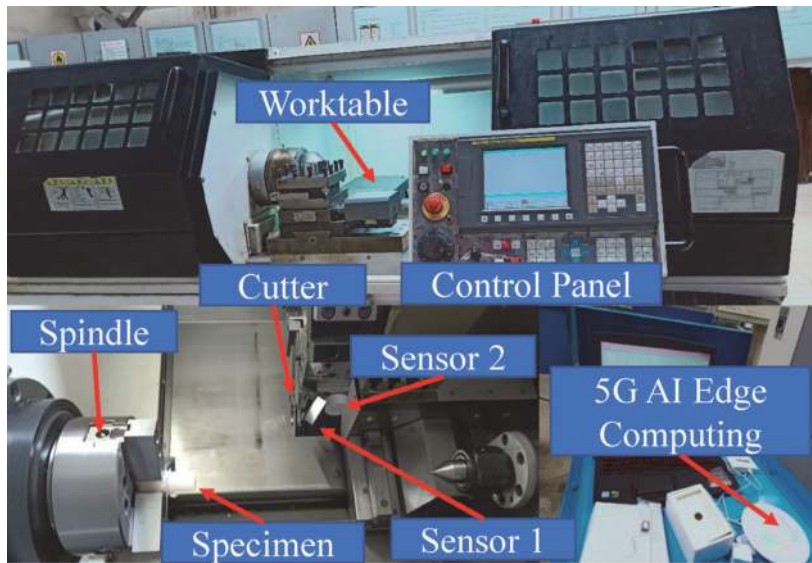


**Figure 22.**  
 Real-time monitoring of the CNC process in a production environment.

S/N	Diameter(mm)	Rotating speed (RPM)	Feed rate (r/min)	Length(mm)
A1	25	100	0.30	30
A2	25	300	0.20	30
A3	25	500	0.10	30
A4	25	700	0.08	30
A5	25	900	0.06	30
A6	25	1100	0.05	30
A7	25	1300	0.05	30
A8	25	1500	0.03	30
A9	25	1700	0.02	30
A10	25	1900	0.01	30

**Table 1.**  
 Group A specimens with varied machining parameters.

When the rotating speed of the main spindle of CNC machine is the same, the same feed rate is selected as well. The feed rate is increased with increasing rotating speed.

**Figure 23** shows three groups of specimens labeled as A1–A10, B1–B10, and C1–C10 respectively. Group A specimens are used as training data set while group B and C specimens are used as testing data set.

### 5.3 Signal processing technologies for processing parameter optimization

There are various signal processing technologies for analyzing the monitoring machine working condition and product processing. The commonly used technologies are: time domain signal processing; FFT; wavelet technology; and short-time Fourier transform (STFT). Normally, time domain data are the original data recorded by the sensor, FFT is the technology developed to convert time domain

S/N	Diameter(mm)	Rotating speed (RPM)	Feed rate (r/min)	Length(mm)
B1	25	100	0.30	30
B2	25	300	0.20	30
B3	25	500	0.10	30
B4	25	700	0.08	30
B5	25	900	0.06	30
B6	25	1100	0.05	30
B7	25	1300	0.05	30
B8	25	1500	0.03	30
B9	25	1700	0.02	30
B10	25	1900	0.01	30

**Table 2.**  
*Group B specimens with varied machining parameters.*

S/N	Diameter(mm)	Rotating speed (RPM)	Feed rate (r/min)	Length(mm)
C1	25	100	0.30	30
C2	25	300	0.20	30
C3	25	500	0.10	30
C4	25	700	0.08	30
C5	25	900	0.06	30
C6	25	1100	0.05	30
C7	25	1300	0.05	30
C8	25	1500	0.03	30
C9	25	1700	0.02	30
C10	25	1900	0.01	30

**Table 3.**  
*Experimental specimen group C with varied machining parameters.*

data to frequency domain data. The wavelet technology is commonly used to decompose a complex signal to sleeve sub-level simple signals. STFT is the signal processing technology developed to overcome the drawbacks of FFT. In most cases, it is used to monitor the transition signal. In this section, each signal technology will be discussed based on experimental data. The purpose is to find out the most suitable signal processing technology to develop process parameter optimization.

Sensor 1 is attached to the tip of the cutter to monitor the cutting dynamic force-induced vibration. The sensor is a wireless accelerometer and powered by a built-in battery. As shown in **Figures 24** and **25**, time domain signal is repeatable with signal noise. However, we cannot trace enough useful information from the signal in time domain.

Due to lack of useful information from time domain data, frequency domain data are converted from time domain data by employing FFT technology. In machine fault diagnosis application, the fault frequencies can be found when the machine is under faulty working condition such as bearing wear and tear.

**Figures 26** and **27** show the frequency domain data of Sensor 1 in X and Y directions, respectively. The domain frequency is the 1x order signal frequency, which is around 31.67 Hz. The second contribution signal is around 263 Hz. The third and fourth ones are that of 2x order and 3x order signal respectively.



**Figure 23.**  
*Experimental specimen groups with varied machining parameters.*

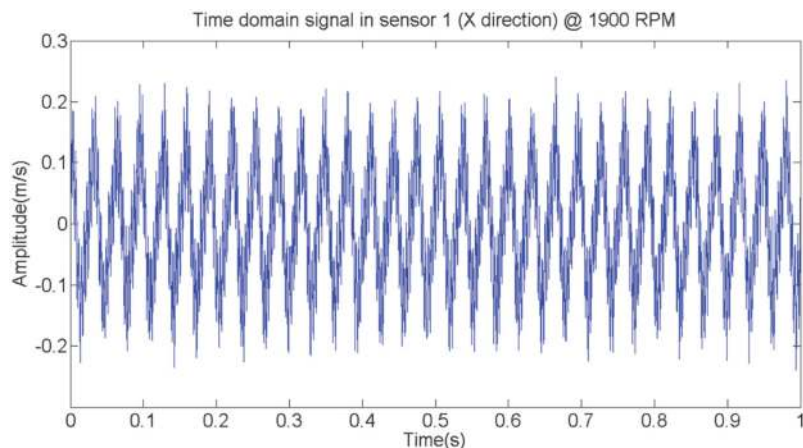


**Figure 24.**  
*Time domain signal in Sensor 1 in X direction.*

Wavelet technology is originally developed to decompose complex signal. It may be used in the processing application to trace useful information. **Figure 28** shows wavelet spectrum in sensor 1 in X and Y directions; it can be seen that the signal is decomposed. However, only first two domain signals can be displayed. Moreover, the frequency of each signal cannot be recognized, which means this signal technology may be not suitable for processing optimization application. Other signal technologies should be further studied to be applied in this application field.

**Figure 29** shows short-time Fourier transform spectrum in sensor 1 in X and Y directions. It can be seen that the dominant signal is the low-frequency component. However, it cannot provide any useful information for optimizing processing parameters. In **Figures 26** and **27**, we know that the dominant frequency is the 1x order of main spindle rotating frequency. Waterfall technology is used to apply FFT in several steps of the main spindle's rotational speed in order to trace any changes due to change in rotating frequency.

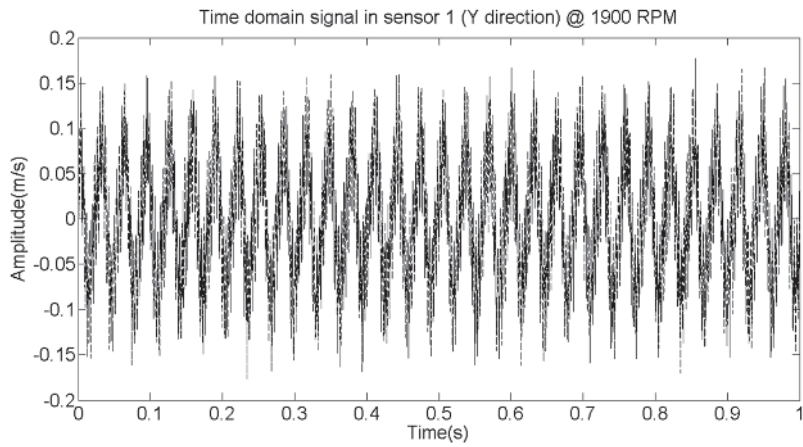


**Figure 25.**  
*Time domain signal in Sensor 1 in Y direction.*

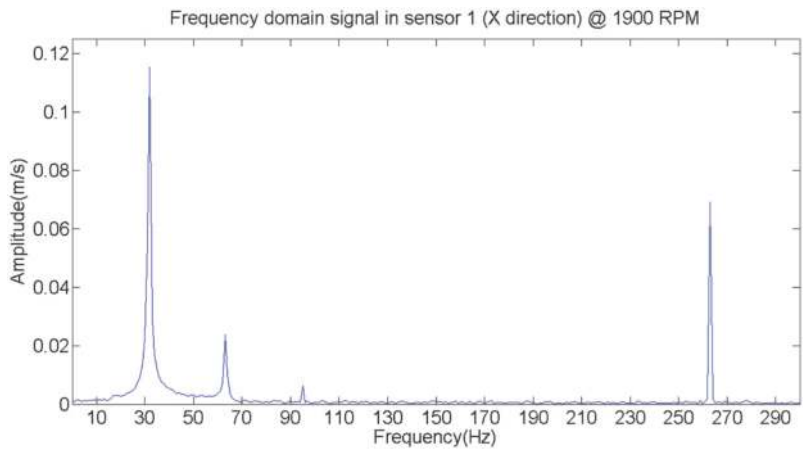


**Figure 26.**  
*Frequency domain signal in Sensor 1 in X direction.*

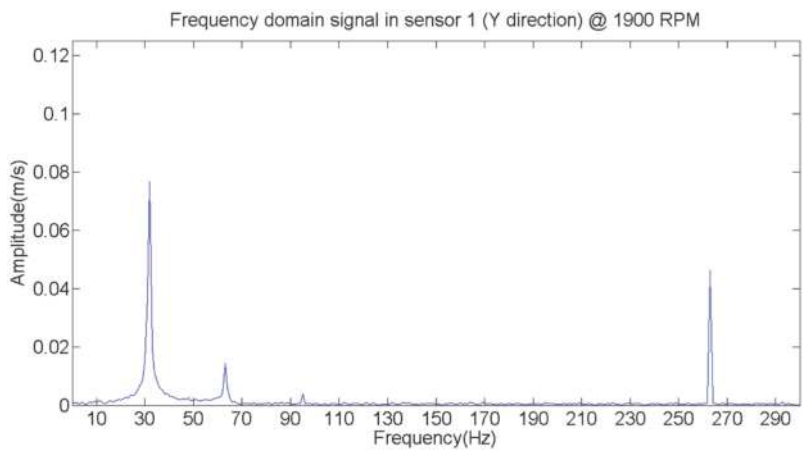


**Figure 27.**  
*Frequency domain signal in Sensor 1 in Y direction.*

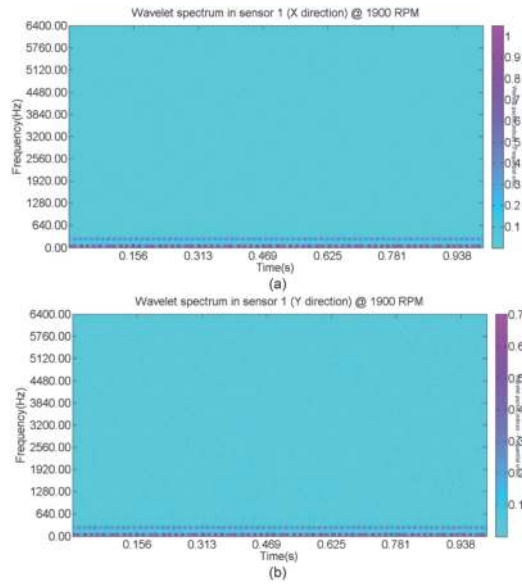


**Figure 28.**  
*Wavelet spectrum in Sensor 1 in X and Y directions.*

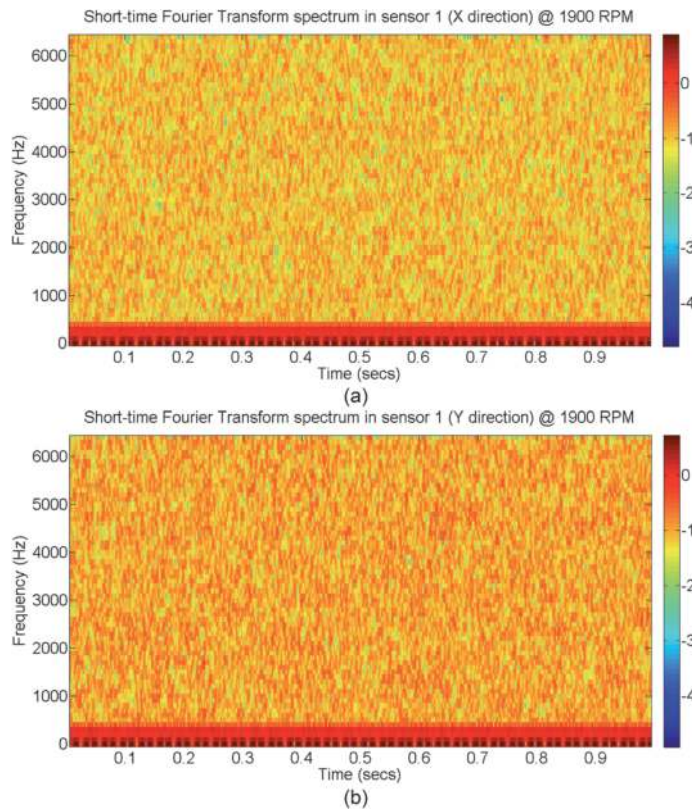


**Figure 29.**  
*Short-time Fourier transform spectrum in Sensor 1 in X and Y directions.*

## 5.4 Experimental results of processing parameter optimization

The useful information is traced when the waterfall of speed spectrum is developed. Sensor 1 is attached to the tip of the cutting tool to monitor the cutting dynamic force-induced vibration. **Figures 30** and **31** show the vibration in X and Y directions

respectively. In **Figure 30**, it can be seen that the dominant frequency components are 1x, 2x, and 3x. Moreover, the maximum value is 0.12 mm/s at 31.6 Hz and the vibration spectrum is increased with increasing rotating speed. The lowest resonance frequency of the CNC machine is 263 Hz. Therefore, the machine rotating speed has to deviate far away from 15,780 rpm.

In **Figure 31**, the maximum value is 0.08 mm/s at 31.6 Hz. Under 1900 rpm, the maximum value is smaller at 31.6 Hz, as the cutter bears bigger cutting force due to removal of material by cutter in X direction.

Sensor 2 is attached to the base of the cutting tool to monitor the cutting dynamic force-induced vibration. **Figures 32 and 33** show the vibration in x and y direction respectively. It can be seen that the maximum vibration of Sensor 2 is 0.025 and 0.16 mm/s in x and y direction respectively, both smaller than that of Sensor 1. Therefore, the vibration signal of Sensor 1 is more sensitive and is a better candidate than Sensor 2 for monitoring the CNC machine working status. Furthermore, only the frequency domain dominates frequencies and their amplitudes are selected to be sent to the cloud in order to reduce data size and increase data transmission rate.

After the speed spectrum is obtained, the frequencies and their peak value can be obtained by applying data mining methodology. **Figure 34** shows the tracing peak

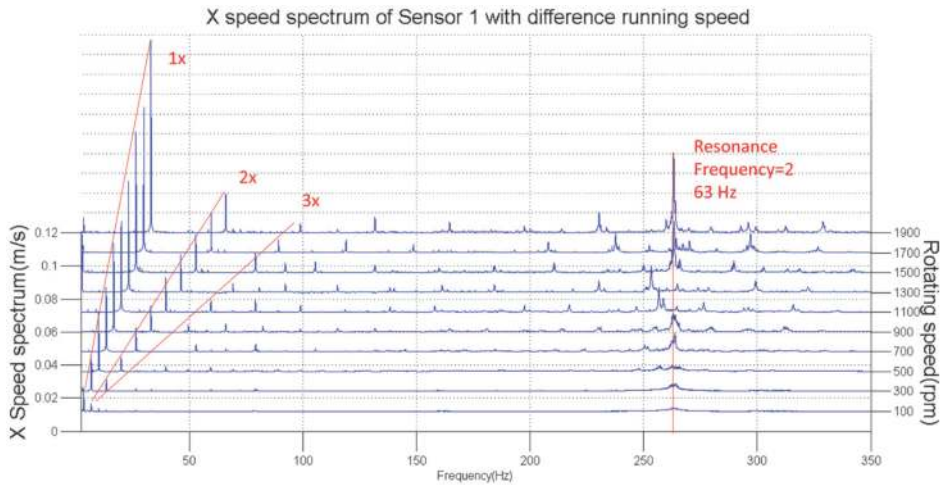


**Figure 30.**  
Vibration signal in X direction of Sensor 1.

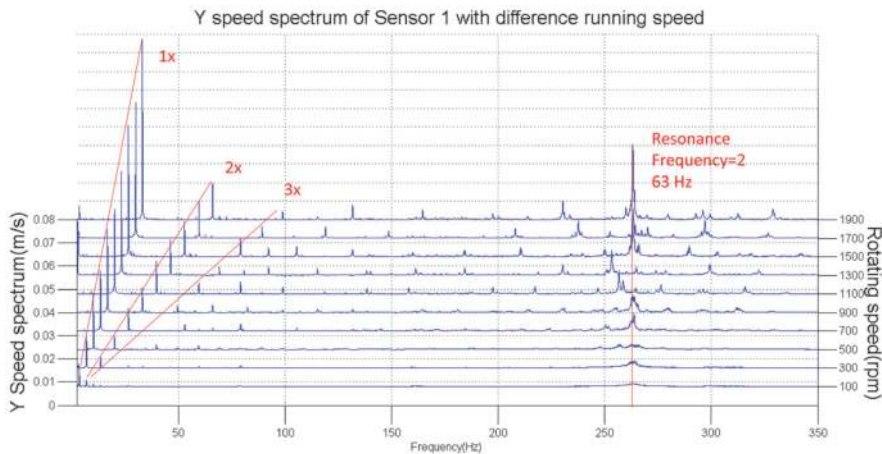


**Figure 31.**  
Vibration signal in Y direction of Sensor 1.



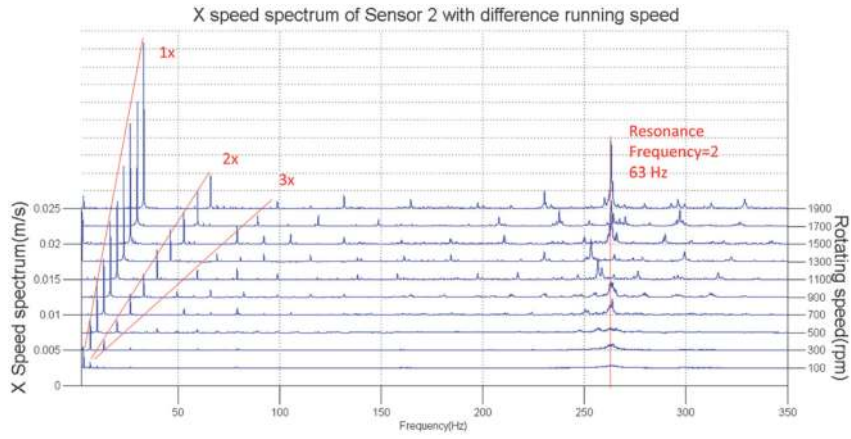


**Figure 32.**  
*Vibration signal in X direction of Sensor 2.*

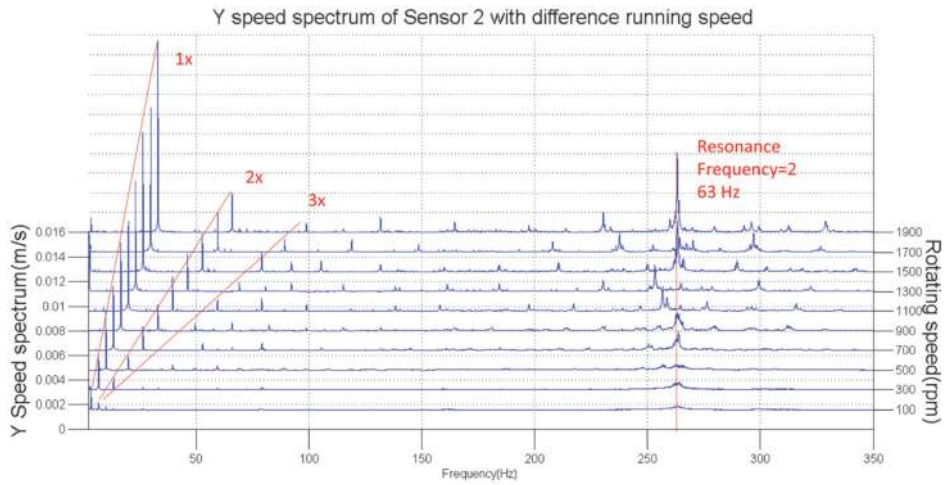


**Figure 33.**  
*Vibration signal in Y direction of Sensor 2.*

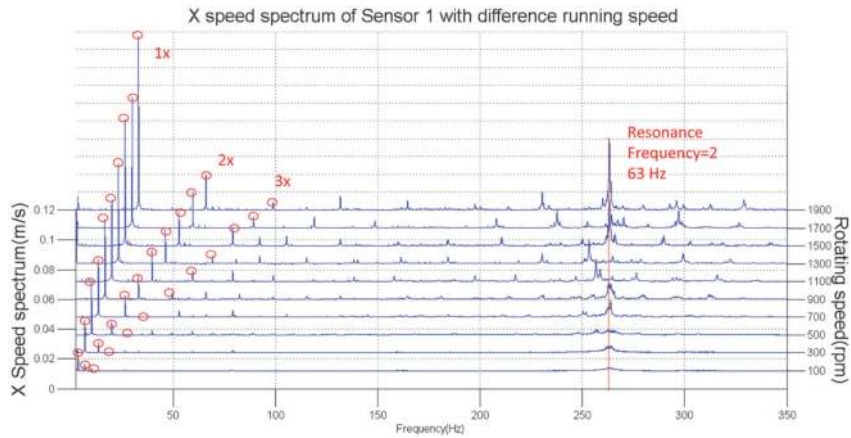


**Figure 34.**  
*Tracing peak values of group a specimens in frequency domain.*

values of group A specimen in frequency domain with interesting 1x, 2x, and 3x data. The peak values of specimen A, B, and C are shown in **Tables 4–6** respectively.

The experimental parameters such as material, dimensions, temperature, reaction forces, vibration data, and machining quality such as tolerances will be sent to the Multilayer Artificial Neural Network (MANN) to train the optimized operation parameters. The MANN is shown in **Figure 35**.

**Figure 36** shows results of MANN training based on training data, the training correction is about 99%. If more training data are adopted, the trained MANN should be more accurate.

**Figure 37** shows general data classification results based on deep learning; there are four types of results: (a) The machining result is linearly classified into two

S/N	Rotating speed (RPM)	1 <sup>st</sup> vibration in X (mm/s)	2 <sup>nd</sup> vibration in X (mm/s)	3 <sup>rd</sup> vibration in X (mm/s)	1 <sup>st</sup> vibration in Y (mm/s)	2 <sup>nd</sup> vibration in Y (mm/s)	3 <sup>rd</sup> vibration in Y (mm/s)
A1	100	0.01349	0.00433	0.001583	0.00899	0.00288	0.001055
A2	300	0.02196	0.00683	0.001353	0.01464	0.00455	0.000189
A3	500	0.03635	0.00834	0.003509	0.02424	0.00566	0.0001864
A4	700	0.03911	0.01471	0.00283	0.02608	0.00981	0.000159
A5	900	0.05354	0.01576	0.004258	0.03569	0.01051	0.002839
A6	1100	0.05495	0.02097	0.006776	0.03663	0.01398	0.004519
A7	1300	0.06709	0.02301	0.005445	0.04473	0.01534	0.003630
A8	1500	0.08472	0.02256	0.01205	0.05661	0.01504	0.008036
A9	1700	0.08787	0.02442	0.007477	0.05858	0.01628	0.003930
A10	1900	0.11650	0.02332	0.005225	0.07771	0.01424	0.003484

**Table 4.**  
*Vibration speed spectrum of group A specimen.*

S/N	Rotating speed (RPM)	1 <sup>st</sup> vibration in X (mm/s)	2 <sup>nd</sup> vibration in X (mm/s)	3 <sup>rd</sup> vibration in X (mm/s)	1 <sup>st</sup> vibration in Y (mm/s)	2 <sup>nd</sup> vibration in Y (mm/s)	3 <sup>rd</sup> vibration in Y (mm/s)
B1	100	0.01227	0.00393	0.001389	0.00856	0.00289	0.000955
B2	300	0.01996	0.00625	0.001356	0.01392	0.00457	0.000159
B3	500	0.03305	0.00768	0.003509	0.02375	0.00522	0.000176
B4	700	0.03556	0.01389	0.003871	0.02548	0.00919	0.000168
B5	900	0.04867	0.01435	0.006163	0.03446	0.00985	0.002762
B6	1100	0.04996	0.01906	0.004949	0.03438	0.01356	0.004327
B7	1300	0.06099	0.02091	0.005445	0.04293	0.01415	0.003403
B8	1500	0.07723	0.02051	0.005691	0.05308	0.01438	0.007534
B9	1700	0.07989	0.02221	0.005377	0.05492	0.01526	0.004673
B10	1900	0.10590	0.02128	0.004725	0.07284	0.01458	0.003266

**Table 5.**  
*Vibration speed spectrum of group B specimen.*

S/N	Rotating speed (RPM)	1 <sup>st</sup> vibration in X (mm/s)	2 <sup>nd</sup> vibration in X (mm/s)	3 <sup>rd</sup> vibration in X (mm/s)	1 <sup>st</sup> vibration in Y (mm/s)	2 <sup>nd</sup> vibration in Y (mm/s)	3 <sup>rd</sup> vibration in Y (mm/s)
C1	100	0.013776	0.004561	0.001615	0.00969	0.00309	0.001135
C2	300	0.022455	0.008512	0.001489	0.01597	0.00483	0.000160
C3	500	0.037152	0.009501	0.003332	0.02594	0.00595	0.000166
C4	700	0.039975	0.016095	0.003891	0.02748	0.01059	0.000168
C5	900	0.054656	0.021396	0.005345	0.03825	0.01259	0.003065
C6	1100	0.056174	0.020348	0.006918	0.03945	0.01489	0.004847
C7	1300	0.068568	0.021915	0.005555	0.04795	0.01645	0.003989
C8	1500	0.086655	0.020513	0.007123	0.06069	0.01668	0.008615
C9	1700	0.089672	0.024926	0.007635	0.06278	0.01756	0.005341
C10	1900	0.118923	0.023856	0.005332	0.08325	0.01569	0.003732

**Table 6.**  
*Vibration speed spectrum of group C specimen.*

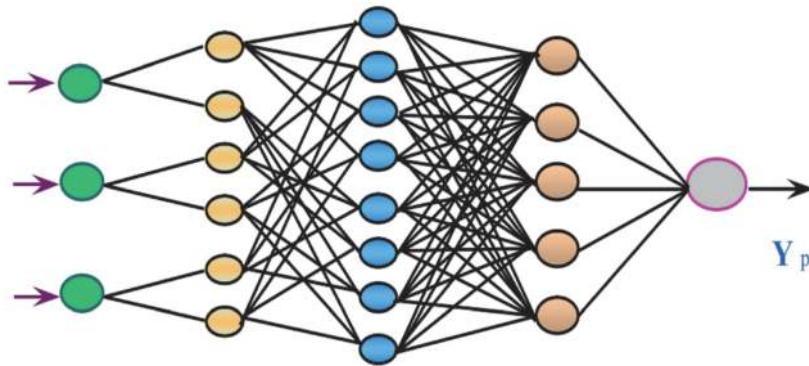


Figure 35.  
 Multilayer artificial neural network (MANN).

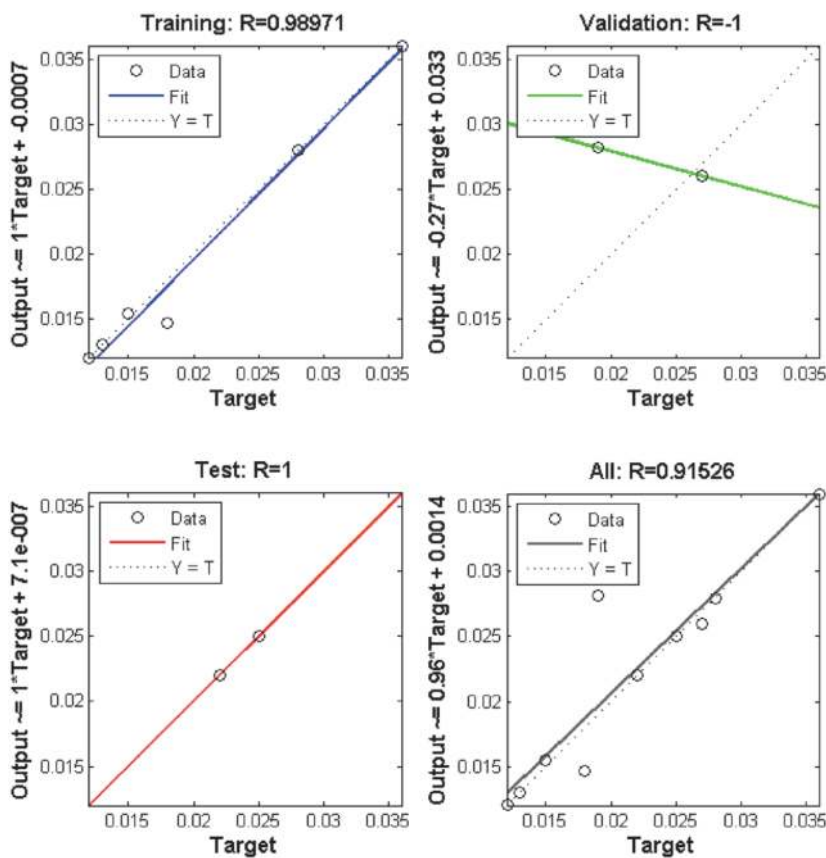
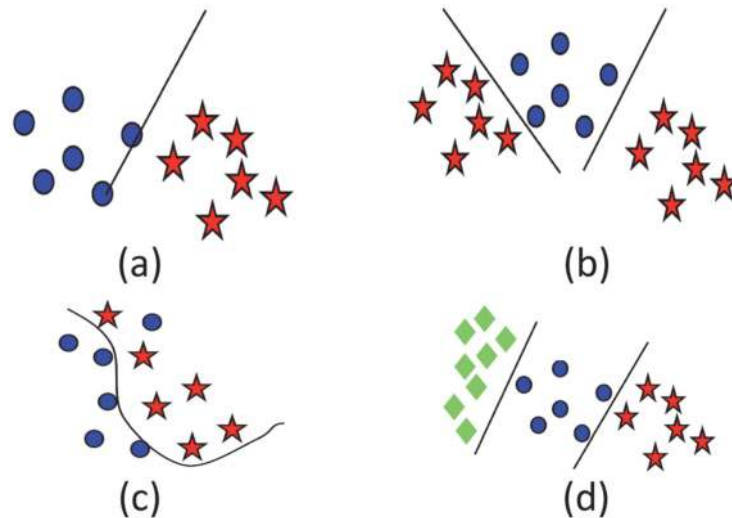
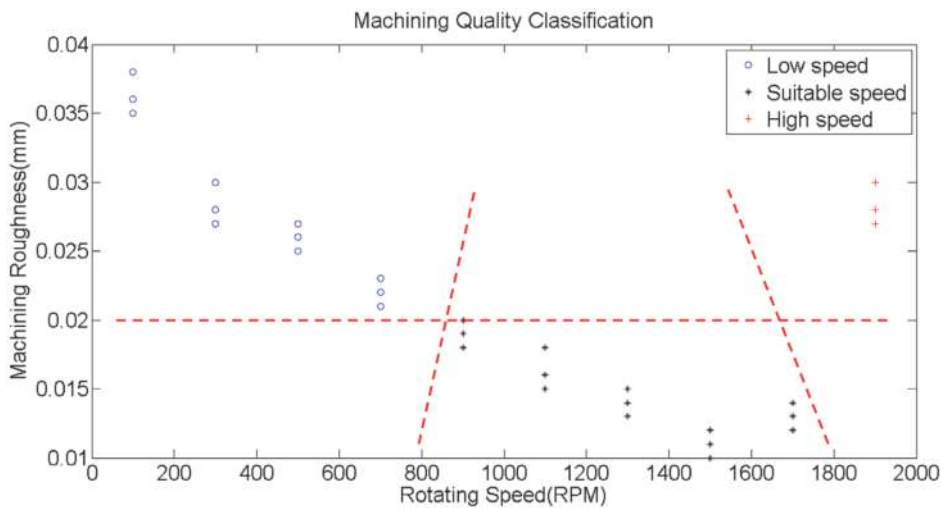


Figure 36.  
 Results of multilayer artificial neural network (MANN) training.

groups: one that met the quality requirements and one that failed to meet the quality requirements. (b) The result is linearly classified into three groups as low, medium, and high rotation speed range. In low and high rang, the machining quality cannot meet the quality requirement. Sometimes, the machining quality classification is not linear as shown in (c). The classification quality is not only based on deep learning technology but also depends on the quantity of parameters and the machining material. The matching quality can be further classified into grades of quality such as grade A, B, and C, as shown in **Figure 36**, based on machining tolerances.



**Figure 37.** Data classification results based on deep learning. (a) Two classes linear classification, (b) multi-classes classification, (c) two classes non-linear classification, and (d) multi-classes non-linear classification.



**Figure 38.** Classification results of machining nylon with varied speed of CNC.

**Figure 38** shows classification results of machining Nylon with variable speed of CNC based on deep learning. If the machining roughness threshold is set as 0.02 mm, the spindle speed of CNC should be more than 900 rpm and less than 1800 rpm.

## 6. Conclusions

This chapter presents our research studies on a parameter optimization method of product processing procedure for CNC machine tool with three common systematic errors compensation approaches.

In Section 1, we introduced mechanism optimization, energy consumption optimization, and processing optimization of a CNC machine tool. Mechanism optimization is mainly used to optimize the CNC machine tool to reduce machine

systematic errors. On the other hand, due to huge electrical energy consumption of CNC machine tool under operational mode, energy consumption optimization should be considered. There are tremendous researches on the first two aspects but less on the last one. Therefore, in the next section, our studies focus on the processing optimization approach.

In Section 2, we briefly introduced the working principle of CNC machine tools. In order to reduce machining error, the cutting force has to be monitored constantly. The machining of the complex surface can be decoupled into simpler ones for path optimization in order to minimize speed fluctuation-induced machining error. For the same purpose, machining tool overcutting compensation and two major indicators  $S_t$  and  $S_q$  of the machining accuracy are introduced and an optimized profile is proposed.

In Section 3, we studied tool deflection issue during machining. The merits and drawback of two commonly used displacement sensors, capacitive probe and eddy current gap sensor, are compared and recommended for different scenarios. In this section, 5G AI edge computing technology for signal pre-processing and genetic programming for control algorithm parameters optimization are proposed. The experimental results with tool deflection compensation are reduced by 40%.

In Section 4, we studied error feedback compensation approach. The CNC and servo actuator are in the close loop for error feedback compensation. A bandpass filter is adopted to reduce the noise in order to reconstruct the control signal. The experimental result is reduced by 60%.

In Section 5, we studied processing parameter optimization. The cloud-based intelligent network configuration for processing parameter optimization is proposed. In this section, the method is mainly based on deep learning approach such as GP, MANN, and SVM to identify the product processing optimized parameters. Before deep learning approach is employed in cloud computing with expert system and database, all the information in the train data instance such as raw material type and dimensions, CNC machine tool systematic parameters, and machining operational conditions and vibration outputs of the CNC machine tool must be sent to a cloud-based computing center. The amplitudes and frequencies of the CNC machine tool outputs are determined by the waterfall of FFT after the signal is pre-processed through 5G AI edge computation. The functionality and performance of the proposed technique are verified with simulations as well as with the experimental data and results, which proves the effectiveness of the proposed scheme.

## **Acknowledgements**

First and foremost, I would like to thank East China Jiao Tong University for providing the research funding (No: 2003419018) for this study. I would like to express my gratitude to Dr. Yang Yang, Director of Engineering Experiment Teaching Center of East China Jiao Tong University, for his invaluable support, Mr. wang Guorong and Ms. Zhang han for their meaningful experimental setup in this study.

I would like to thank for all the help I received from my colleagues, Dr. Liu Yande, Dr. Hu Guoliang, Dr. Zhou Jianming, Dr. Chen Qiping and Dr. Tu Wenbing, from School of Mechatronics & Vehicle Engineering in East China Jiao Tong University, who helped me one way or another.

Finally, I would like to thank my son, Mr. Yu Shi Jie, for improving the writing of this document and my family for their unwavering support.

## **Author details**


YinQuan Yu

East China Jiao Tong University, Nan Chang, Jiang Xi Province, China

\*Address all correspondence to: [yu\\_yinquan@ecjtu.edu.cn](mailto:yu_yinquan@ecjtu.edu.cn)

## **IntechOpen**

---

© 2020 The Author(s). Licensee IntechOpen. Distributed under the terms of the Creative Commons Attribution - NonCommercial 4.0 License (<https://creativecommons.org/licenses/by-nc/4.0/>), which permits use, distribution and reproduction for non-commercial purposes, provided the original is properly cited. 

## References

- [1] Shukun C, Heng Z, Xiangbo Z, Qiujuan Y, Changsheng A. Software and hardware platform design for open-CNC system. In: 2008 IEEE International Symposium on Knowledge Acquisition and Modeling Workshop; 21–22 December 2008; Wuhan. New York: IEEE; 2008. pp. 139-142. DOI: 10.1109/KAMW.2008.4810444
- [2] Prado Y, Valiño G, Blanco D, Suárez CM, Álvarez BJ. Models for stiffness characterization of the spindle-chuck system in a CNC lathe for prediction of deflections in CAPP. In: 2010 IEEE 15th Conference on Emerging Technologies & Factory Automation (ETFA 2010); 13–16 September 2010; Bilbao. New York: IEEE; 2010. pp. 1-7. DOI: 10.1109/ETFA.2010.5641361
- [3] Yang Y et al. Geometric error modeling and compensation of the dual-driving feed worktable. In: 2019 6th International Conference on Systems and Informatics (ICSAI); 2–4 November 2019; Shanghai. New York: IEEE; 2020. pp. 86-91. DOI: 10.1109/ICSAI48974.2019.9010391
- [4] Gang L, He X. Analysis on the basic application technology of CNC machine tools. *China New Technology & Products*. 2019;23:94-95. DOI: 10.1590/S0100-73862002000300009
- [5] Chen G, Liang Y, Sun Y, Chen W, Wang B. Volumetric error modeling and sensitivity analysis for designing a five-axis ultra-precision machine tool. *International Journal of Advanced Manufacturing Technology*. 2013;68: 2525-2534. DOI: 10.1007/s00170-013-4874-4
- [6] Gabriel S, Raul C. Gouveia R. designing a novel feeding system for CNC turning machines. *Procedia Manufacturing*. 2018;17:1144-1153. DOI: 10.1016/j.promfg.2018.10.020
- [7] Lin Z, Guo R, Chen L, Geng C, Wang F. Design and development of the self-adaptive tool path decision-making CNC platform. In: 2012 International Conference on Biomedical Engineering and Biotechnology; 28–30 May 2012; Macao. New York: IEEE; 2012. pp. 135-137. DOI: 10.1109/iCBEB.2012.126
- [8] Lapsomthop O, Wongsirirax N, Kititeerakol A, Sawangri W. Design and experimental investigation on 3-component force sensor in mini CNC milling machine. *Materials Today: Proceedings*. 2019;17(4):1931-1938. DOI: 10.1016/j.matpr.2019.06.232
- [9] Moreira LC, Li WD, Lu X, Fitzpatrick ME. Supervision controller for real-time surface quality assurance in CNC machining using artificial intelligence. *Computers and Industrial Engineering*. 2019;127:158-168. DOI: 10.1016/j.cie.2018.12.016
- [10] Cheng Q, Zhao H, Zhao Y, et al. Machining accuracy reliability analysis of multi-axis machine tool based on Monte Carlo simulation. *Journal of Intelligent Manufacturing*. 2018;29: 191-209. DOI: 10.1007/s10845-015-1101-1
- [11] Xie C, Zhang WM, He XY. Kinematic analysis and post-processing algorithm research for 5-axis CNC machine tools with a universal head. In: 2009 IEEE International Conference on Industrial Engineering and Engineering Management; 8–11 December 2009; Hong Kong. New York: IEEE; 2009. pp. 2309-2313. DOI: 10.1109/IEEM.2009.5373031
- [12] Cortina M, Arrizubieta JI, Ruiz JE, Ukar E, Lamikiz A. Latest developments in industrial hybrid machine tools that combine additive and subtractive operations. *Materials (Basel)*. 2018; 11(12):2583. DOI: 10.3390/ma11122583

- [13] Wang K-C. Optimal high-rigidity structure design for CNC machine tools using CAE technique. *Engineering Computations*. 2014;**31**(8):1761-1777. DOI: 10.1108/EC-11-2012-0296
- [14] Yang J, Mayer JRR, Altintas Y. A position independent geometric errors identification and correction method for five-axis serial machines based on screw theory. *International Journal of Machine Tools and Manufacture*. 2015; **95**:52-66. DOI: 10.1016/j.ijmactools.2015.04.011
- [15] Zhu X, Bao J, Wang J, Chen F, Li X, Zhang X. A comprehensive maintainability evaluation methods for subsystems of CNC machine tools. *Journal of Physics: Conference Series*. 2018;**1074**:012144. DOI: 10.1088/1742-6596/1074/1/012144
- [16] Zhaojun Y, Dong Z, Chuanhai C, et al. Reliability modelling of CNC machine tools based on the improved maximum likelihood estimation method. *Mathematical Problems in Engineering*. 2018;**2018**:1-11. DOI: 10.1155/2018/4260508
- [17] Li C, Zhang X, Zhang Q, Li H. Numerical simulation analysis of temperature field for motorized spindle of high-grade CNC machine tool based on ANSYS. *Key Engineering Materials*. 2010;**455**:33-36. DOI: 10.4028/www.scientific.net/KEM.455.33
- [18] Vicente García J. Development of Valid Models for Structural Dynamic Analysis [thesis]. South Kensington, London, United Kingdom: Imperial College London; 2008
- [19] Bonte MHA, Fourment L, Do T, et al. Optimization of forging processes using finite element simulations. *Structural and Multidisciplinary Optimization*. 2010;**42**:797-810. DOI: 10.1007/s00158-010-0545-3
- [20] Erfei L, Xinghua N, Yiguang S, Guo Y. Study on the reason of static stiffness of the whole machine in non-circular phenomenon when vertical machining center milling circle. *IOP Conference Series: Materials Science and Engineering*. 2018;**452**:042038. DOI: 10.1088/1757-899X/452/4/042038. 15–16 September 2018; Melbourne
- [21] Bosetti P, Bruschi S. Enhancing positioning accuracy of CNC machine tools by means of direct measurement of deformation. *International Journal of Advanced Manufacturing Technology*. 2012;**58**:5-8. DOI: 10.1007/s00170-011-3411-6
- [22] Kumar V, Kumar BJK, Rudresha N. Optimization of machining parameters in CNC turning of stainless steel (EN19) by Taguchi's orthogonal array experiments. *Materials Today: Proceedings*. 2018;**5**:11395-11407. DOI: 10.1016/j.matpr.2018.02.107
- [23] Shaoke W, Xiaoliang J, Kumar MN, Jun H. Effect of vibration assistance on chatter stability in milling. *International Journal of Machine Tools and Manufacture*. 2019;**145**:103432. DOI: 10.1016/j.ijmactools.2019.103432
- [24] Lee K, Lee T, Yang M. Tool wear monitoring system for CNC end milling using a hybrid approach to cutting force regulation. *International Journal of Advanced Manufacturing Technology*. 2007;**32**:8-17. DOI: 10.1007/s00170-005-0350-0
- [25] Zhang C, Guo S. Error compensation model considering tool wear in milling difficult to cut materials. *International Journal of Computer Integrated Manufacturing*. 2017;**30**(8): 822-838. DOI: 10.1080/0951192X.2016.1210232
- [26] Andrew W. An Early Warning Monitoring System for CNC Spindle Bearing Failure [thesis]. Tigerprints: Clemson, South Carolina, United States: Clemson University; 2011



- [27] Oral A, Cakir MC. Automated cutting tool selection and cutting tool sequence optimisation for rotational parts. *Robotics and Computer-Integrated Manufacturing*. 2004;**20**: 127-141. DOI: 10.1016/j.rcim.2003.10.006
- [28] Han J, Wu L, Yuan B, Tian X, Xia L. A novel gear machining CNC design and experimental research. *The International Journal of Advanced Manufacturing Technology*. 2017;**88**:5-8. DOI: 10.1007/s00170-016-8883-y
- [29] Yang X-Y, Tang J-Y. Research on manufacturing method of CNC plunge milling for spur face-gear. *Journal of Materials Processing Technology*. 2014; **214**:3013-3019. DOI: 10.1016/j.jmatprotec.2014.07.010
- [30] Xing Y, Wang T. Accuracy enhancement in manufacture of spiral bevel gear with multi-axis CNC machine tools by a new compensation method. In: 2011 International Conference on Consumer Electronics, Communications and Networks (CECNet); 11–13 March 2005; Xianning. New York: IEEE; 2011. pp. 3891-3894. DOI: 10.1109/CECNET.2011.5768862
- [31] Lee S-Y. In-process tool condition monitoring systems in CNC turning operations [Thesis]. Ames, Iowa, United States: Iowa State University; 2006
- [32] Smith GC. Using microwave Doppler radar in automated manufacturing applications [Thesis]. Ames, Iowa, United States: Iowa State University; 2004
- [33] Renn JC, Hsu WJ, Liao WC. Energy efficient lathe turret design using load sensing control scheme. In: 2014 International Symposium on Computer, Consumer and Control. 10–12 June 2014, Taiwan. New York: IEEE; 2014. pp. 51-54. DOI: 10.1109/IS3C.2014.26
- [34] Altıntaş RS, Kahya M, Ünver HÖ. Modelling and optimization of energy consumption for feature based milling. *International Journal of Advanced Manufacturing Technology*. 2016;**86**: 3345-3363. DOI: 10.1007/s00170-016-8441-7
- [35] Guoyong Z, Chunhong H, Jianfang Q, Cheng X. Energy consumption characteristics evaluation method in turning. *Advances in Mechanical Engineering*. 2016;**8**(11):1-8. DOI: 10.1177/1687814016680737
- [36] Lv L, Deng Z, Liu T, Wan L, Huang W, Yin H, et al. A composite evaluation model of sustainable manufacturing in machining process for typical machine tools. *Processes*. 2019;**7** (2):110. DOI: 10.3390/pr7020110
- [37] Liu ZJ, Sun DP, Lin CX, Zhao XQ, Yang Y. Multi-objective optimization of the operating conditions in a cutting process based on low carbon emission costs. *Journal of Cleaner Production*. 2016;**124**:266-275. DOI: 10.1016/j.jclepro.2016.02.087
- [38] Jianmai S, Zhong L, Luohao T, Jian X. Multi-objective optimization for a closed-loop network design problem using an improved genetic algorithm. *Applied Mathematical Modelling*. 2017; **45**:14-30. DOI: 10.1016/j.apm.2016.11.004
- [39] Böllinghaus T et al. *Manufacturing Engineering*. Springer Handbook of Mechanical Engineering. Berlin/ Heidelberg: Springer; 2009. pp. 523-785
- [40] Makhanov SS. Adaptable geometric patterns for five-axis machining: A survey. *International Journal of Advanced Manufacturing Technology*. 2010;**47**:1167-1208. DOI: 10.1007/s00170-009-2244-z
- [41] Wasif M, Iqbal SA, Ahmed A, et al. Optimization of simplified grinding wheel geometry for the accurate

generation of end-mill cutters using the five-axis CNC grinding process.

International Journal of Advanced Manufacturing Technology. 2019;**105**: 4325-4344. DOI: 10.1007/s00170-019-04547-8

[42] Mou W, Jiang Z, Zhu S. A study of tool tipping monitoring for titanium milling based on cutting vibration. The International Journal of Advanced Manufacturing Technology. 2019;**104**: 3457-3471. DOI: 10.1007/s00170-019-04059-5

[43] Umbrello D, Jawahir IS. Numerical modeling of the influence of process parameters and workpiece hardness on white layer formation in AISI 52100 steel. International Journal of Advanced Manufacturing Technology. 2009;**44**: 955-968. DOI: 10.1007/s00170-008-1911-9

[44] Reyes Uquillas DA, Yeh S. Tool holder sensor design for measuring the cutting force in CNC turning machines. In: 2015 IEEE International Conference on Advanced Intelligent Mechatronics (AIM); 7–11 July 2015; Busan. New York: IEEE; 2015. pp. 1218-1223. DOI: 10.1109/AIM.2015.7222705

[45] Fountas NA, Vaxevanidis NM, Stergiou CI, et al. A virus-evolutionary multi-objective intelligent tool path optimization methodology for 5-axis sculptured surface CNC machining. Engineering with Computers. 2017;**33**: 375-391. DOI: 10.1007/s00366-016-0479-5

[46] Du X, Sun Y. Dynamic transmission error analysis for CNC machine tools under variable speed condition. In: 2018 IEEE 4th Information Technology and Mechatronics Engineering Conference (ITOEC), 14–16 December 2018; Chongqing. New York: IEEE; 2018. pp. 113-120. DOI: 10.1109/ITOEC.2018.8740694

[47] Patil RS, Jadhav SM. Boring parameters optimization for minimum surface roughness using CNC boring

machine with passive damping material. In: 2017 2nd International Conference for Convergence in Technology (I2CT), 7–9 April 2017; Mumbai. New York: IEEE; 2017. pp. 300-303. DOI: 10.1109/I2CT.2017.8226140

[48] Nie X. Application of neural network for thermal error compensation in CNC machine tool. In: 2011 IEEE 2nd International Conference on Computing, Control and Industrial Engineering, 20–21 August 2011; Wuhan. New York: IEEE; 2011. pp. 211-215. DOI: 10.1109/CCIENG.2011.6007995

[49] Bobyr MV, Abduldaiem AN, Abduljabbar MA. Cooled cutter control algorithm based on fuzzy logic. In: 2017 International Conference on Industrial Engineering, Applications and Manufacturing (ICIEAM), 16–19 May 2017; St. Petersburg. New York: IEEE; 2017. pp. 1-5. DOI: 10.1109/ICIEAM.2017.8076168

[50] Liu J et al. Thermal boundary condition optimization of ball screw feed drive system based on response surface analysis. Mechanical Systems and Signal Processing. 2019;**121**:471-495. DOI: 10.1016/j.ymssp.2018.11.042

[51] Jie G, Agapiou JS, Kurgin S. Global offset compensation for CNC machine tools based on Workpiece errors. Procedia Manufacturing. 2016;**5**: 442-454. DOI: 10.1016/j.promfg.2016.08.037

[52] Béres M, Paripás B. Measurements of vibration by laser doppler method in the course of drilling. In: Jármai K, Bolló B, editors. Vehicle and Automotive Engineering. Lecture Notes in Mechanical Engineering. Vol. 2. Cham: Springer; 2018. DOI: 10.1007/978-3-319-75677-6\_16

[53] Li X et al. Monocular-vision-based contouring error detection and compensation for CNC machine tools. Precision Engineering. 2019;**55**:447-463. DOI: 10.1016/j.precisioneng.2018.10.015